

MASTER'S THESIS

INVESTIGATION OF PROTON INDUCED REACTIONS  
IN LIGHT NUCLEI USING PROPORTIONAL COUNTER

CAPTAIN J. O. F. DORSETT, USN  
THE OHIO STATE UNIVERSITY

1952

Thesis  
D66

THESIS  
D66



11-27  
200

INVESTIGATION OF PROTON INDUCED REACTIONS IN LIGHT  
NUCLEI USING PROPORTIONAL COUNTER

Abstract of

A Thesis

Presented in Partial Fulfillment of the Requirements  
for the Degree Master of Science

By

JOHN ORIN FILLMORE DORSETT, B.S., M.S. (Met.)

The Ohio State University

1952

Approved by:

\_\_\_\_\_  
Adviser



INVESTIGATION OF PROTON INDUCED REACTIONS IN LIGHT  
NUCLEI USING PROPORTIONAL COUNTER

John Grem Fillmore Dorsett

B. S., U.S. Naval Academy, 1937

M. S., (Met.) Massachusetts Institute of Technology, 1940

Department of Physics

(Approved by James C. Harris)

The general problem was to utilize a proportional counter for observing nuclear reactions induced in proton bombardments by The Ohio State University Van de Graaff electrostatic generator.

The proportional counter, designed by Commander A. B. Chilton, was modified and improved by the addition of a reaction collimator and electrostatic shield between the sensitive volume and reaction chamber. The particular problem investigated was the elastic scattering of protons by argon gas. The gaseous target and filling gas of the counter were the same: 90% argon and 10%  $\text{CO}_2$  under 50 mm. (Hg) pressure. Scattering angle in the laboratory system was  $150^\circ$ . A proton beam current of about 0.2 - 0.3 microamperes was integrated in cycles of 10.9 microcoulombs. or about 6000 counts per minute.

Elastic scattering rate was investigated for proton

INVESTIGATION OF PROTON INDUCED REACTIONS IN LIQUID  
NUCLEI USING PROPORTIONAL COUNTER

John Owen Wilmore Dorence

B. S., U.S. Naval Academy, 1937

M. S., (Met.) Massachusetts Institute of Technology, 1943

Department of Physics

(Approved by James O. Haxby)

The general problem was to utilize a proportional counter for observing nuclear reactions induced in proton bombardments by The Ohio State University Van de Graaff electrostatic generator.

The proportional counter, designed by Commander A. B. Chilton, was modified and improved by the addition of a reaction cell and electrostatic shield between the sensitive volume and reaction chamber. The particular problem investigated was the elastic scattering of protons by argon gas. The gaseous target and filling gas of the counter were the same: 90% argon and 10% CO<sub>2</sub> under 80 mm. (Hg) pressure. Scattering angles in the laboratory system was 150°. A proton beam current of about 0.2 - 0.3 microamperes was integrated in cycles of 10.9 microseconds or about 6000 counts per minute.

Elastic scattering rate was investigated for proton



reaction energies from 710 to 1133 kev. The general trend followed closely the predicted scattering obtained by adding the cross-sections due to Coulomb potential and that due to a hard sphere type of scattering. A definite anomaly was observed at  $908 \pm 10$  kev. Since the experimental resolution was of the order of 20 kev., no attempt was made to compute the resonance width from the energy spread of the extrema. A second run confirmed the existence and shape of the anomaly. The energy of this resonance in  $K^{41}$  agrees closely with investigations made by Broström, Hans, and Koch in 1948 (Nature 162, 695.)

resonance energies from 710 to 1135 Kev. The General trend followed closely the predicted scattering obtained by adding the cross-section due to Coulomb potential and that due to a hard sphere type of scattering. A definite anomaly was observed at 908  $\pm$  10 Kev. Since the experimental resolution was of the order of 30 Kev., no attempt was made to compare the resonance width from the energy spread of the extreme. A second run confirmed the existence and shape of the anomaly. The energy of this resonance in  $K$  agrees closely with investigations made by Broekx, Huns, and Koch in 1949 (Nature 162, 41).



INVESTIGATION OF PROTON INDUCED REACTIONS IN LIGHT  
NUCLEI USING PROPORTIONAL COUNTER

A Thesis

Presented in Partial Fulfillment of the Requirements  
for the Degree Master of Science

By

JOHN ORREN WILLMORE DORSETT, B.S., M.S. (Met.)

The Ohio State University

1952

Approved by:

---

Adviser

INVESTIGATION OF THEORETICAL PROBLEMS IN LIGHT

OF THE THEORY OF THE PROBABILITIES

OF THE THEORY OF THE PROBABILITIES

OF THE THEORY OF THE PROBABILITIES

OF THE THEORY OF THE PROBABILITIES

OF THE THEORY OF THE PROBABILITIES

OF THE THEORY OF THE PROBABILITIES

OF THE THEORY OF THE PROBABILITIES

OF THE THEORY OF THE PROBABILITIES

OF THE THEORY OF THE PROBABILITIES

OF THE THEORY OF THE PROBABILITIES

OF THE THEORY OF THE PROBABILITIES

BY

JOHN EDWIN WILLIAMS, B.A., M.A. (Oxon.)

The Ohio State University

1922

Approved by:

Adviser

#### ACKNOWLEDGMENTS

To Dr. James C. Harris particular thanks are due for suggesting the problem and for his continual advice and encouragement through the trials of getting all apparatus to function smoothly and simultaneously. I wish to thank Commander Arthur B. Shilton for his original design and construction of the proportional counter and his advice in operating the equipment, and Dr. John H. Cooper for his words of encouragement, his interest in the problem, and advice in operation of the Van De Graaff generator. Finally, I would like to thank Messrs. Otis Campbell and Ignace Balduke for technical assistance in operation of the Van De Graaff.

This work was carried out under the auspices of the United States Naval Postgraduate School at Monterey, California.

APPENDIX

Dr. James O. Harris' personal papers are the

the following: his papers and his correspondence; his  
the following: his papers and his correspondence; his  
the following: his papers and his correspondence; his  
the following: his papers and his correspondence; his

the following: his papers and his correspondence; his

the following: his papers and his correspondence; his

the following: his papers and his correspondence; his

the following: his papers and his correspondence; his

the following: his papers and his correspondence; his

the following: his papers and his correspondence; his

and reference is made to the Von de Walle.

This was the first and under the sanction of

the United States Army, the School of Medicine,

California.

TABLE OF CONTENTS

	<u>Page</u>
I. GENERAL	1
II. HISTORICAL AND BACKGROUND	3
III. THE ELASTIC SCATTERING PROBLEM	10
IV. APPARATUS: DESCRIPTION, CALIBRATION, BASIC CALCULATIONS	27
V. EXPERIMENTAL RESULTS	49
VI. SUGGESTIONS FOR FUTURE USE OF APPARATUS	57
VII. TABLES	59
BIBLIOGRAPHY	65

APPENDIX B

1976

1	1976-1977
2	1977-1978
3	1978-1979
4	1979-1980
5	1980-1981
6	1981-1982
7	1982-1983
8	1983-1984
9	1984-1985
10	1985-1986
11	1986-1987
12	1987-1988
13	1988-1989
14	1989-1990
15	1990-1991
16	1991-1992
17	1992-1993
18	1993-1994
19	1994-1995
20	1995-1996
21	1996-1997
22	1997-1998
23	1998-1999
24	1999-2000
25	2000-2001
26	2001-2002
27	2002-2003
28	2003-2004
29	2004-2005
30	2005-2006
31	2006-2007
32	2007-2008
33	2008-2009
34	2009-2010
35	2010-2011
36	2011-2012
37	2012-2013
38	2013-2014
39	2014-2015
40	2015-2016
41	2016-2017
42	2017-2018
43	2018-2019
44	2019-2020
45	2020-2021
46	2021-2022
47	2022-2023
48	2023-2024
49	2024-2025
50	2025-2026
51	2026-2027
52	2027-2028
53	2028-2029
54	2029-2030
55	2030-2031
56	2031-2032
57	2032-2033
58	2033-2034
59	2034-2035
60	2035-2036
61	2036-2037
62	2037-2038
63	2038-2039
64	2039-2040
65	2040-2041
66	2041-2042
67	2042-2043
68	2043-2044
69	2044-2045
70	2045-2046
71	2046-2047
72	2047-2048
73	2048-2049
74	2049-2050
75	2050-2051
76	2051-2052
77	2052-2053
78	2053-2054
79	2054-2055
80	2055-2056
81	2056-2057
82	2057-2058
83	2058-2059
84	2059-2060
85	2060-2061
86	2061-2062
87	2062-2063
88	2063-2064
89	2064-2065
90	2065-2066
91	2066-2067
92	2067-2068
93	2068-2069
94	2069-2070
95	2070-2071
96	2071-2072
97	2072-2073
98	2073-2074
99	2074-2075
100	2075-2076



## I. GENERAL

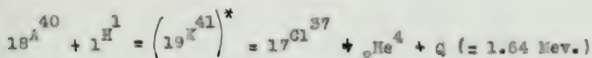
The problem in general was to investigate certain proton induced reactions using a sensitive and highly discriminating proportional counter. The Van de Graaff generator at The Ohio State University provides a source of protons of fairly discrete energies within the range of 0.3 and 1.5 Mev. The reactions induced in targets made of various materials were to be detected by means of a sensitive proportional counter. When used with a linear amplifier having a discriminating circuit, a method was provided for detecting and discriminating between proton groups or between protons and alpha particles.

Originally, it was planned to investigate the (p- $\alpha$ ) reactions in light nuclei using as a target very thin nickel or copper foil. Difficulties were encountered in monitoring the beam with a solid target installed, especially since the beam current had to be kept down to the order of 0.1 microampere to avoid saturating the counter with recoil protons. Suggestions for correcting this difficulty are discussed in Section VI. Pending further modification of the target assembly, it was decided to investigate elastic scattering from the argon used as a counting gas in the chamber. This type of experiment per-



mitted visual monitoring of the beam while using low beam currents.

Two possibilities were recognized: (1) anomalies in the elastic scattering would indicate resonances in  $\Lambda$  and (2) a low energy (p- $\alpha$ ) reaction is energetically possible from atomic mass considerations with  $Q = +1.64$  Mev. The chance that the latter reaction might have a large cross-section was deemed to be very remote because of the high Coulomb barrier of argon to both incident and emitted particles. The reaction is as follows:



The (p-n) reaction for  $\Lambda^{40}$  was ruled out on account of a negative  $Q$  of approximately -1.7 Mev.

... ..  
 ... ..

The ... ..  
 ... ..  
 ... ..  
 ... ..  
 ... ..  
 ... ..  
 ... ..  
 ... ..

... .. The version is as follows:

$$P(x) = \frac{1}{2} \left( \frac{1}{2} \right)^x + \frac{1}{2} \left( \frac{1}{2} \right)^{x+1} + \dots$$

... ..  
 ... ..  
 ... ..

## II. KINETICAL AND DYNAMIC ASPECTS

Scattering phenomena belong to one of three general classes:

- (1) Elastic (Coulomb or Rutherford) scattering.
- (2) Inelastic scattering.
- (3) Resonance scattering.

### Elastic Scattering.

Elastic scattering occurs when the kinetic energy of the system is conserved. In the case of a fast light particle "colliding" with a heavy slow moving particle the light particle has almost the same energy after collision as before. Rutherford's original theory of the atomic nucleus was verified by experiments in which the elastic scattering of  $\alpha$ -particles from thin gold foils was observed. He assumed that the positive charge of the gold nucleus was concentrated in a small volume which contained most of the atomic mass. This charge was considered as a point charge whose electric field satisfied the Coulomb law of repulsion. The exact deflection of small positive charges such as alphas would depend on the initial path of the particle with respect to the bombarded nucleus. Elastic scattering will be covered in greater detail in the next section.

### Inelastic Scattering.

If the incident particle penetrates within the Coulomb barrier so that the short range nuclear forces come into

THE HISTORY OF THE

... ..

...

(1) ... ..

(2) ... ..

(3) ... ..

...

... ..

... .. In the case of a ... ..

... .. with a ... ..

... ..

... ..

... ..

... ..

... ..

... ..

... ..

... ..

... ..

... ..

... ..

... ..

...

... ..

... ..



play, kinetic energy and momentum will not be separately conserved. Some of the particle energy is transferred to the nucleus which goes to an excited quantum state. The transferred energy is emitted as a gamma photon when the nucleus, after emitting a particle of the same kind as the incident particle, returns to the ground state again. Such a process is inelastic scattering. The problem of inelastic scattering has been treated by Born<sup>1</sup> as a perturbation problem in quantum mechanics.

Inelastic scattering of protons has been investigated by several workers: Bieke and Marshall (1945)<sup>2</sup>; Wilkins (1941)<sup>3</sup>; Davis and Haffner (1948)<sup>4</sup>; Powell, May, Chadwick and Pickavance (1940)<sup>5</sup>; Fulbright and Bush (1948)<sup>6</sup>; and Thoderick (1950)<sup>7</sup>.

Whereas, elastically scattered charged particles are scattered mainly in the forward direction, inelastically scattered particles tend to a symmetrical angular distribution. This indicates the formation of a compound nucleus from which the entering particle is re-emitted with spherical symmetry.

Inelastic scattering of protons may be thought of as a (p,p) reaction in which the proton leaves with a lower kinetic energy. The scattering nucleus is raised to an excited state at the expense of the kinetic energy of the system. Observation of the energy spectrum of the scattered protons

with the electric energy is transformed in  
 the electric energy is transformed in  
 the electric energy is transformed in  
 the electric energy is transformed in  
 the electric energy is transformed in  
 the electric energy is transformed in  
 the electric energy is transformed in  
 the electric energy is transformed in  
 the electric energy is transformed in  
 the electric energy is transformed in

the electric energy is transformed in  
 the electric energy is transformed in  
 the electric energy is transformed in  
 the electric energy is transformed in  
 the electric energy is transformed in  
 the electric energy is transformed in  
 the electric energy is transformed in  
 the electric energy is transformed in  
 the electric energy is transformed in  
 the electric energy is transformed in

the electric energy is transformed in  
 the electric energy is transformed in  
 the electric energy is transformed in  
 the electric energy is transformed in  
 the electric energy is transformed in  
 the electric energy is transformed in  
 the electric energy is transformed in  
 the electric energy is transformed in  
 the electric energy is transformed in  
 the electric energy is transformed in

gives information of the nuclear levels involved. Before interpretation can be made of the results, the possibility of such a reaction as that shown in Fig. 1(b) must be excluded.<sup>7</sup>

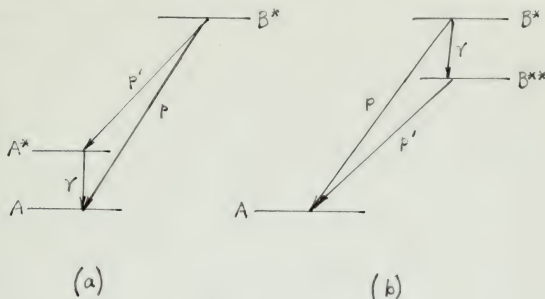


Fig. 1.

The process diagrammed in Fig. 1(b) produces inelastically scattered protons but does not involve any excited states of the residual nucleus. Rhoderick<sup>7</sup> states that the probability at most of such a process taking place is only one-thousandth as great as that of a direct transition to the ground state of  $B$ . This is far less probable than simple capture, which in turn is far less likely than emission of a proton, because of the smallness of the radiative width of nuclear levels. We can therefore assume that inelastic scattering follows the pattern of



Fig. 1(a), and therefore the loss of energy of the proton (in the center-of-mass system) is equal to the excitation energy of the residual nucleus.

Wicks and Marshall<sup>2</sup> point out that (p,n) reactions are much more likely than (p,p) reactions due to the Coulomb barrier. Thus, if the (p,n) reaction is energetically possible, one would expect very little (n,p) inelastic reactions. Substances most suitable for inelastic proton scattering are those with high (p,n) thresholds and these are found mostly in light nuclei.

Powell, et al<sup>3</sup>, obtained information on probability of scattering at angles of  $15^\circ$  through  $150^\circ$ . Inelastically scattered protons from neon were found to be distributed with spherical symmetry. No inelastic protons were observed in oxygen up to 4 Mev. Chlorine and argon were investigated and the ratio of inelastic to elastic scattering was very much smaller than in the case of neon corresponding to the decreased probability of protons entering the nucleus with increasing nuclear charge.

When the bombarding particle penetrates the nuclear barrier to form a compound nucleus, the scattering ceases to be purely elastic and becomes a transmutation process. Historically, the first of these processes<sup>4</sup> was Rutherford's bombardment of nitrogen in 1919 with alpha particles to form oxygen in the ground state with the emission of a proton. The equation for this reaction is:

like this, and therefore, the same is true of the other

and the same is true of the other

and the same is true of the other

and the same is true of the other

and the same is true of the other

and the same is true of the other

and the same is true of the other

and the same is true of the other

and the same is true of the other

and the same is true of the other

and the same is true of the other

and the same is true of the other

and the same is true of the other

and the same is true of the other

and the same is true of the other

and the same is true of the other

and the same is true of the other

and the same is true of the other

and the same is true of the other

and the same is true of the other

and the same is true of the other

and the same is true of the other

and the same is true of the other

and the same is true of the other

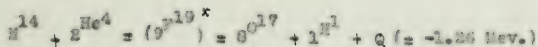
and the same is true of the other

and the same is true of the other

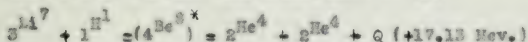
and the same is true of the other

and the same is true of the other





The first successful disintegration utilizing protons was performed by Crocker and Walton in 1932.<sup>9</sup> Protons were accelerated in a hydrogen discharge tube up to 0.5 Mev. and used to bombard lithium; alpha particles were observed on a fluorescent screen. The reaction<sup>10,11</sup> is:



This reaction has now been studied by many observers and is as well known as to be a calibrating reaction.

Other important (p- $\alpha$ ) reactions summarized by Livingston and Bethe in Rev. Mod. Phys. 9, 311 (1937) were reported by: Heuvert<sup>11</sup>; Kirchner and Heuvert<sup>12</sup>; Oliphant, Kempton, and Rutherford<sup>13</sup>; Dee and Gilbert<sup>14</sup>; and Henderson, Livingston, and Lawrence<sup>15</sup>.

### Resonance Phenomena

At certain proton energies the probability that the excitation energy of the compound nucleus is close to one of the quantum states is high. The probability of the formation of the compound nucleus, therefore is great. Such a condition is called resonance. It corresponds to the excitation of a mechanical system when an impressed force oscillates with a frequency near the mechanical resonant frequency.<sup>16</sup>

Resonances may be observed in several ways. One way is

$$T_{\text{end}} = 23.0 \pm 0.2 \text{ K}, \quad T_{\text{beg}} = 7.7 \pm 0.2 \text{ K}, \quad T_{\text{mid}} = 15.3 \pm 0.2 \text{ K}$$

Example 2. Let  $\mathcal{A} = \{A_1, A_2, A_3, A_4, A_5, A_6, A_7, A_8, A_9, A_{10}\}$

to note the disappearance of incident particles, that is, a peak in the cross-section for capture. Another method is to look for increased effects associated with the formation of a compound nucleus. These would be a peak in either gamma emission or production of some other particle than the incident particle such as the  $(p-\alpha)$ ,  $(d-\alpha)$ ,  $(p-n)$ ,  $(n-p)$ , etc. Still another method is to observe anomalies in the elastic scattering of protons of which more will be said in the next section.

If gamma rays only are observed, i.e. heavy particle emission is impossible, the quantum (or excited) state is called a bound state. If particles can be emitted ( $p$ ,  $\alpha$ , or  $n$ ) however, the state is called a virtual state. Energy levels in light nuclei are beginning to be fairly well known and have been reviewed and summarized by various writers.<sup>17,18</sup>

Devons<sup>19</sup> states that observation of discrete resonances in nuclei of  $Z > 30$  is not likely since the proton energy for appreciable yields ( $\sim 3$  Mev.) corresponds to an excitation energy of the compound nucleus in excess of 10 Mev. at which energies the level spacing of quantum states is probably less than any energy resolution experimentally attainable.

The mean life of an excited state is related to the level width by the uncertainty relation:

$$\Gamma \tau = \frac{h}{2\pi} \quad \text{where} \quad \begin{array}{l} \Gamma = \text{level width} \\ \tau = \text{mean life} \\ h = \text{Planck's constant} \end{array}$$

This says that well defined states have long lifetimes, and

It is noted that the above information is being furnished to the Bureau for its information and for its use in the event of a future investigation of the activities of the Communist Party, U.S.A. and its branches and affiliates.

conversely. With the high excitations necessary for heavy nuclei, the levels become wider than the mean interval between neighboring levels. Proton resonances have been observed only for nuclei of  $Z$  up to 20, the processes observed were  $(p, \gamma)$ ,  $(p, \alpha)$  and elastic scattering.

Freeman and Baxter<sup>23</sup> found  $(p, \alpha)$  resonances in  $\text{Na}^{23}$  at proton energies of 590, 750, 800, and 910 Kev. with  $Q = 2.14$  Mev. and  $\text{Al}^{27}$  at proton energies of 650, 730, and 920 Kev. with  $Q = 1.32$  Mev.

Resonances in  $\text{K}^{41}$  due to proton bombardment of  $\text{A}^{40}$  have been reported by Brostrom, Huus, and Koch<sup>21</sup> as follows:

$E_p$ (Kev.)	900	1050	1080	1100	1235
$\gamma - \gamma_0$	0.2	0.4	0.5	1.0	3.5

where  $\gamma - \gamma_0$  = difference between resonance yield,  $\gamma$ , in counts/ $\mu\text{C}$ . and background,  $\gamma_0$ , which was about 0.1 for all resonances.

Proton scattering experiments using the Van de Graaff generator as a source provides a means for initiating resonance phenomena. Observation of these furnishes information on the excited states of the compound nucleus. Some of the results obtainable from the study of resonance peaks are:

- (1) Energy of excited states,
- (2) Mean life of excited states,
- (3) Interference between excited states, and
- (4) Modes of decay of excited states.

...the ... of the ...  
 ...the ... of the ...  
 ...the ... of the ...  
 ...the ... of the ...

...the ... of the ...  
 ...the ... of the ...  
 ...the ... of the ...

...the ... of the ...  
 ...the ... of the ...  
 ...the ... of the ...

...the ... of the ...  
 ...the ... of the ...  
 ...the ... of the ...

...the ... of the ...  
 ...the ... of the ...  
 ...the ... of the ...

...the ... of the ...  
 ...the ... of the ...  
 ...the ... of the ...



### III. THE ELASTIC SCATTERING PROBLEM.

As stated in Section II, elastic scattering occurs when the kinetic energy of the system is conserved. For a pure Coulomb potential,  $V(r) \sim \frac{1}{r}$ , Rutherford derived from purely classical considerations a formula for the differential cross-section:

$$\sigma_d(\theta) = \left[ \frac{zZe^2}{4E} \right]^2 \frac{1}{\sin^4\left(\frac{\theta}{2}\right)}$$

where  $\theta$  = scattering angle (deviation)  
 $e$  = electronic charge  
 $z$  = atomic no. of incident particle  
 $Z$  = atomic no. of scattering nucleus  
 $E$  = kinetic energy of incident particle

Being a long range type of potential,  $\sigma_d(\theta)$  is strongly dependent on the angle of scattering. Figure 2 is a plot of the factor:  $\frac{1}{\sin^4\left(\frac{\theta}{2}\right)}$  showing that Coulomb (Rutherford)

$$\frac{1}{\sin^4\left(\frac{\theta}{2}\right)}$$

scattering is mostly in the forward direction.

Landé<sup>22</sup> treats the problem from a wave mechanical point of view where a modified Coulomb potential<sup>23</sup> is considered as a perturbation.

The modified potential is:  $V'(r) = \frac{zZe^2}{r} \exp\left(-\frac{r}{r_0}\right)$  where

where  $r_0$  is a parameter which limits the Coulomb force.

Such a modified potential actually exists for charged particles scattered by neutral atoms. The solution of this

Published Weekly, excepting the Fourth Week of December, When It Appears Twice a Week

Subscription Price, Five Dollars per Annum in Advance

Single Copies, Fifteen Cents

Entered as Second-Class Matter, October 3, 1917, Post Office at Chicago, Ill., under No. 100,000

Acceptance for mailing at special rate of postage provided for in Act of October 3, 1917

$$\frac{1}{2} \left( \frac{1}{2} + \frac{1}{2} \right) = 1$$

There is a general feeling of dissatisfaction among the medical profession with the present state of affairs in the medical profession. The feeling is based upon many factors, and it is the purpose of this paper to discuss some of the most important of these factors.

The first factor is the question of the medical profession's position in the community. The medical profession has long been a part of the community, and it has always been a part of the community. But in recent years, the medical profession has become more and more isolated from the community.

The second factor is the question of the medical profession's position in the medical profession. The medical profession has long been a part of the medical profession, and it has always been a part of the medical profession. But in recent years, the medical profession has become more and more isolated from the medical profession.

The third factor is the question of the medical profession's position in the medical profession. The medical profession has long been a part of the medical profession, and it has always been a part of the medical profession. But in recent years, the medical profession has become more and more isolated from the medical profession.

The fourth factor is the question of the medical profession's position in the medical profession. The medical profession has long been a part of the medical profession, and it has always been a part of the medical profession. But in recent years, the medical profession has become more and more isolated from the medical profession.

The fifth factor is the question of the medical profession's position in the medical profession. The medical profession has long been a part of the medical profession, and it has always been a part of the medical profession. But in recent years, the medical profession has become more and more isolated from the medical profession.

The sixth factor is the question of the medical profession's position in the medical profession. The medical profession has long been a part of the medical profession, and it has always been a part of the medical profession. But in recent years, the medical profession has become more and more isolated from the medical profession.

The seventh factor is the question of the medical profession's position in the medical profession. The medical profession has long been a part of the medical profession, and it has always been a part of the medical profession. But in recent years, the medical profession has become more and more isolated from the medical profession.

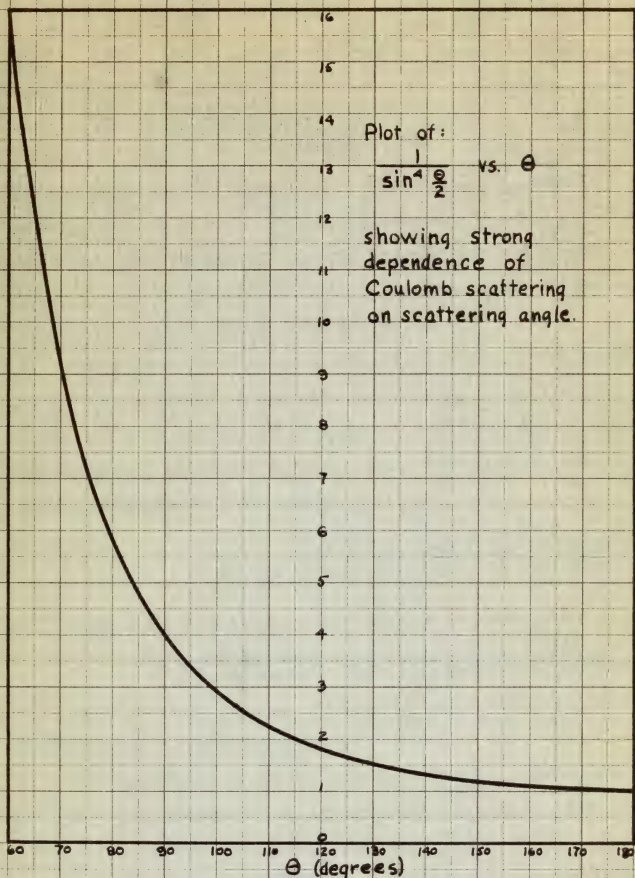


FIGURE 2



yields a cross-section which has a finite value at  $\theta = 0$ , viz.,

$$\sigma_s(\theta) = \left[ \frac{zZe^2}{4E \sin^2 \frac{\theta}{2} + \frac{(\hbar)^2}{(Emv_{\theta} r_0)^2}} \right]^2$$

When  $r_0 = \infty$ , the formula is the same as the Rutherford formula, but for finite  $r_0$ ,  $\sigma_s(\theta)$  remains finite at  $\theta = 0$ .

The above formulae apply for scattering of protons by large nuclei but not for proton-proton scattering due to the "exchange" forces between like particles.

The differential cross-section is a ratio of the number of particles scattered per unit solid angle (steradian) in the direction  $\theta$  to the number of incident particles per unit area. The number of particles per unit solid angle,  $n(\theta)$ , scattered in the direction  $\theta$  is therefore:

$$n(\theta) = n_0 N t \sigma_s(\theta) \quad \left[ \text{This assumes that multiple scattering is small and that the scattering centers do not shield one another.} \right]$$

where  $n_0$  = initial no. of incident particles

$N$  = no. of scattering atoms per unit volume

$t$  = thickness of scattering medium (linear units)

In estimating cross-section for elastic scattering three factors must be considered:

- (1) Modification of the incident beam by the Coulomb field before reaching the nuclear forces. (Rutherford scattering.)
- (2) Potential scattering by a specifically nuclear field

which is a representation which has a finite value at  $\theta = 0$ .

$$\tau(\theta) = \left[ \frac{e^{\theta} \left( \frac{1}{\theta} + \frac{1}{\theta^2} \right)}{1 + \frac{1}{\theta}} \right]$$

For  $\theta \rightarrow \infty$ , the term  $\frac{1}{\theta}$  in the denominator of the fraction

vanishes, and the term  $\frac{1}{\theta^2}$  in the numerator vanishes, so that

the limit of  $\tau(\theta)$  as  $\theta \rightarrow \infty$  is  $e$ .

It is not difficult to see that  $\tau(\theta)$  is a decreasing function of  $\theta$ .

It is also not difficult to see that  $\tau(\theta)$  is a concave down function of  $\theta$ .

The following table gives the values of  $\tau(\theta)$  for various values of  $\theta$ .

It is seen from the table that  $\tau(\theta)$  is a decreasing function of  $\theta$ .

It is also seen from the table that  $\tau(\theta)$  is a concave down function of  $\theta$ .

The values of  $\tau(\theta)$  for various values of  $\theta$  are given in the following table.

It is seen from the table that  $\tau(\theta)$  is a decreasing function of  $\theta$ .

It is also seen from the table that  $\tau(\theta)$  is a concave down function of  $\theta$ .

The values of  $\tau(\theta)$  for various values of  $\theta$  are given in the following table.

It is seen from the table that  $\tau(\theta)$  is a decreasing function of  $\theta$ .

It is also seen from the table that  $\tau(\theta)$  is a concave down function of  $\theta$ .

The values of  $\tau(\theta)$  for various values of  $\theta$  are given in the following table.

It is seen from the table that  $\tau(\theta)$  is a decreasing function of  $\theta$ .

It is also seen from the table that  $\tau(\theta)$  is a concave down function of  $\theta$ .

The values of  $\tau(\theta)$  for various values of  $\theta$  are given in the following table.

It is seen from the table that  $\tau(\theta)$  is a decreasing function of  $\theta$ .

It is also seen from the table that  $\tau(\theta)$  is a concave down function of  $\theta$ .

The values of  $\tau(\theta)$  for various values of  $\theta$  are given in the following table.

It is seen from the table that  $\tau(\theta)$  is a decreasing function of  $\theta$ .

of force.

(3) Scattering in which a compound nucleus is formed.

Using the Rutherford formula and assuming our detecting apparatus counts scattered protons at a constant angle,  $\theta_0$ , from the incident beam, we can plot the no. of scattered protons as functions of beam energy. Using arbitrary units for counting rate of 100 protons/sec. at an energy of 1 Mev. the relation is:

$$n(E) = \frac{100}{E^2} \quad (\text{protons/sec.})$$

This curve is plotted in Figure 5.

Anomalies or deviations from the counting rate predicted by the Rutherford formula will be found for certain energies of the incident particle depending on factors (2) and (3) above. If the energy of the incident proton plus the energy of the scattering nucleus is equal to the energy of one of the quantum states of the compound nucleus, anomalous scattering will occur. Wirt<sup>24</sup> states that anomalous scattering that increases slowly with increasing particle energy indicates penetration of the nuclear barrier; and anomalous scattering that increases rapidly to a maximum and then decreases as the energy is further increased indicates resonance scattering.

#### Resonance Scattering.

In order to see what these anomalies in Rutherford

(b) The Committee is of the opinion that the information  
 furnished by the Government is not reliable and should not be  
 used for any purpose. The Committee is of the opinion that the  
 information furnished by the Government is not reliable and should  
 not be used for any purpose. The Committee is of the opinion that  
 the information furnished by the Government is not reliable and  
 should not be used for any purpose. The Committee is of the  
 opinion that the information furnished by the Government is not  
 reliable and should not be used for any purpose. The Committee  
 is of the opinion that the information furnished by the Govern-  
 ment is not reliable and should not be used for any purpose.

$$m(t) = \frac{1}{2} (p(t) + q(t))$$

and the result is given in Table 1. The result is given in  
 Table 1. The result is given in Table 1. The result is given  
 in Table 1. The result is given in Table 1. The result is  
 given in Table 1. The result is given in Table 1. The result  
 is given in Table 1. The result is given in Table 1. The  
 result is given in Table 1. The result is given in Table 1.  
 The result is given in Table 1. The result is given in Table  
 1. The result is given in Table 1. The result is given in  
 Table 1. The result is given in Table 1. The result is given  
 in Table 1. The result is given in Table 1. The result is  
 given in Table 1. The result is given in Table 1. The result  
 is given in Table 1. The result is given in Table 1. The  
 result is given in Table 1. The result is given in Table 1.  
 The result is given in Table 1. The result is given in Table  
 1. The result is given in Table 1. The result is given in  
 Table 1. The result is given in Table 1. The result is given  
 in Table 1. The result is given in Table 1. The result is  
 given in Table 1. The result is given in Table 1. The result  
 is given in Table 1. The result is given in Table 1. The  
 result is given in Table 1. The result is given in Table 1.

SECRET

It is to be noted that the information is not reliable



Dependence of Coulomb Scattering on Energy at  
a fixed angle of scattering  $\theta$ .

$$n(E) = \frac{100}{E^2} \text{ (arbitrary units)}$$

100 units at 1 Mev.

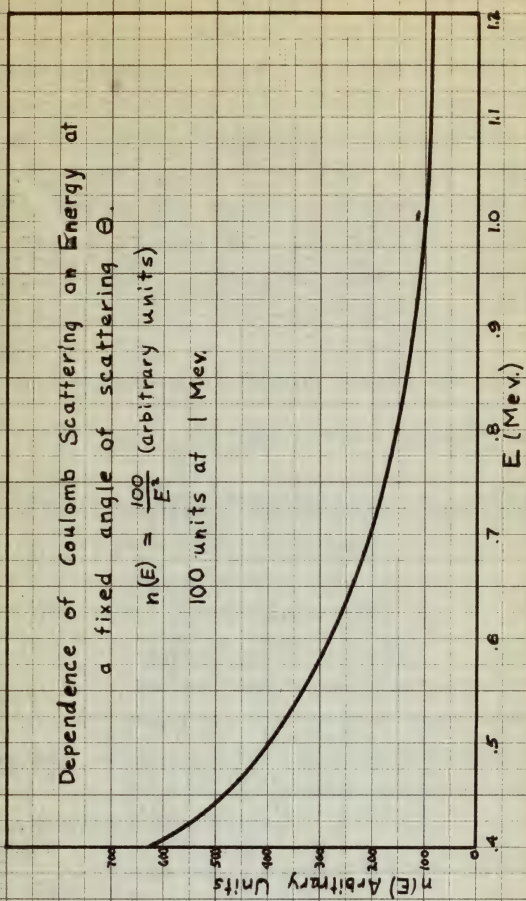


FIGURE 3.



scattering consist of, it is necessary to look at resonance scattering and nuclear potential scattering. The former occurs when the compound nucleus is formed in an excited state, the latter occurs in that region where the nuclear forces are felt by the incident particle but without the formation of a compound nucleus. For protons on nuclei of much heavier mass, nuclear potential scattering can be considered as small compared to pure Coulomb scattering. For neutrons, however, potential scattering by the nuclear forces is a large factor.

Feshbach, et al.<sup>25</sup> using Breit-Wigner theory, develop a formula for elastic scattering cross-section near a resonance level for particles of angular momentum zero ( $l = 0$ ):

$$\sigma_{sc} = \frac{\lambda^2}{\pi} \left| \frac{\Gamma_a}{2(E - E_0) + i\Gamma} + e^{2\pi i a/\lambda} \sin\left(\frac{2\pi a}{\lambda}\right) \right|^2$$

where:  $\Gamma_a$  = partial level width due to the reemission of a particle like the incident particle.

$\Gamma$  = total width of resonance.

$a$  = nuclear radius

$E_0$  = energy at resonance

$E$  = energy of incident particle

$\lambda$  = deBroglie wave length of incident particle

The first term between the bars represents the resonance scattering, the second represents the potential scattering. If only potential scattering were present, the scattering cross-section would be given by:

$$\sigma_{pot} = \frac{\lambda^2}{\pi} \sin^2\left(\frac{2\pi a}{\lambda}\right) \quad \text{which is the scattering due to}$$

1. The first step is to identify the problem or goal. This involves understanding the current situation and what needs to be achieved. It is important to be clear and specific about the objectives.

[illegible]

$$\frac{d}{dt} \left( \frac{\partial L}{\partial \dot{x}} \right) = \frac{\partial L}{\partial x} + \frac{\partial L}{\partial t}$$

\*800000000 10 000000000

✓ = herbicide was longer or indeterminate

0701-0401 for words be given by:

$$\left( \frac{\partial \bar{G}}{\partial \lambda} \right)_{T,P} = \frac{\Delta}{\Delta \lambda} = \Delta G$$

an impenetrable sphere of radius  $a$ .

If potential scattering is neglected, the cross-section becomes that due to a single resonance level:

$$\sigma_{\text{res}} = \frac{\lambda^2}{\pi} \cdot \frac{\Gamma_a^2}{4(E - E_0)^2 + \Gamma^2}$$

Since the magnitude of the potential scattering depends on the term:  $\sin\left(\frac{E_0 a}{\lambda}\right)$ , it can be assumed that it is negligible at low proton energies due to the increasing value of  $\lambda$ . At proton energies above 0.7 Mev. it does become appreciable; the nuclear radius for  $A^{40}$  computed from:  $a = 1.5 A^{1/3} \times 10^{-13}$  cm. is:  $a = 3.15 \times 10^{-13}$  cm. and  $\lambda = 2.91 \times 10^{-12}$  cm. for a Mev. proton from which the value of  $\sin\left(\frac{E_0 a}{\lambda}\right)$  is 0.836 and  $\sin^2\left(\frac{E_0 a}{\lambda}\right) = 0.795$ .

The combined effects, however, include cross-terms which represent interference phenomena between resonance and potential scattering. At certain phase relations between the two waves, destructive interference occurs and at others, constructive interference occurs.

If there are only two possible outcomes of a nuclear collision, for example, re-emission of the incident particle or formation of a compound nucleus with emission of a different particle, then we speak of partial disintegration constants,  $\Gamma_a$  and  $\Gamma_b$ . These are partial level widths for the two competitive processes and the total level width is simply:

7-1-74

$$\Gamma = \Gamma_a + \Gamma_b.$$

If, however, there are other possible ways for the compound nucleus to break up then the total width is:

$\Gamma = \Gamma_a + \Gamma_b + \sum_x \Gamma_x$ , where  $\Gamma_x$  refers to all the other possible modes of disintegration.

For the reaction,



the Breit-Wigner cross-section for emission of particle of type b is given by:

$$\sigma_{AB} = \frac{\lambda^2}{\pi} \cdot \frac{\Gamma_a \Gamma_b}{4(E - E_0)^2 + \Gamma^2}$$

This assumes zero angular momentum of the compound nucleus, i.e.  $l = 0$ , and neglects effects due to spin of particles.

### Interference between Resonance Scattering and Coulomb Scattering.

Detection of resonance scattering in the presence of strong Coulomb scattering may be extremely difficult. Devons<sup>19</sup> gives a very simple method for estimating the conditions under which it is possible.

If we assume that no other process than resonance scattering has comparable probability at resonance then we may set  $\Gamma = \Gamma_0$  and  $E = E_0$ . The resonance differential cross-section then reduces to:

$$L = L_0 + L_1$$

It is, however, clear that the results of the present study are not in agreement with the results of the previous studies.

The results of the present study are in agreement with the results of the previous studies.

The results of the present study are in agreement with the results of the previous studies.

$$L = L_0 + L_1$$

The results of the present study are in agreement with the results of the previous studies.

$$L = L_0 + L_1$$

The results of the present study are in agreement with the results of the previous studies.

# CONCLUSIONS

The results of the present study are in agreement with the results of the previous studies.

The results of the present study are in agreement with the results of the previous studies.



$$\sigma_{\text{res}} = \frac{\lambda_a^2}{4\pi^2} = \frac{h^2}{2 m v_0^2}$$

This neglects angular momentum of the compound state and intrinsic angular momenta of the initial nucleus and incident proton. A spin-statistical factor of order unity,  $g$ , is introduced by Fermi<sup>26</sup>, viz.,

$$g = \frac{1}{2} \left( 1 + \frac{1}{2 I_A + 1} \right), \text{ where } \begin{array}{l} I_A = \text{spin of scattering nucleus} \\ \frac{1}{2} = \text{spin of proton} \end{array}$$

and spin of the compound nucleus,  $I_C = I_A \pm \frac{1}{2}$ .

Then, the resonance cross-section is:

$$\sigma_{\text{res}} = g \cdot \frac{h^2}{2 m v_0^2}$$

Representative values of  $g$  are:

$I_A$	0	$+\frac{1}{2}$	$-\frac{1}{2}$	+1	-1
$g$	1.0	$\frac{3}{4}$	(Indet.)	$\frac{5}{8}$	0.1

The ratio of resonance scattering to Coulomb scattering at resonance is then:

$$\begin{aligned} \frac{\sigma_r(\theta)}{\sigma_c(\theta)} &= g \cdot \frac{8 E_0 K^2}{n (2 e^2)^2} \sin^4 \left( \frac{\theta}{2} \right) \quad \text{where } n = \text{reduced mass of proton} \\ &= 3.8 \times 10^3 \cdot \frac{E_0}{E^2} \sin^4 \left( \frac{\theta}{2} \right) \quad \begin{array}{l} E = \text{resonance energy in Mev.} \end{array} \\ &\text{assuming } g = 1. \end{aligned}$$

In practice, this ratio will be further reduced by a factor,  $\frac{\Gamma_r}{\delta E}$  if the level width,  $\Gamma_r$ , is less than the

$$\frac{h}{m\lambda} = \frac{h}{m\lambda_0} \sqrt{1 - \frac{v^2}{c^2}}$$

The relativistic mass of the electron is given by the expression  $m = \frac{m_0}{\sqrt{1 - \frac{v^2}{c^2}}}$  where  $m_0$  is the rest mass of the electron and  $v$  is its velocity. The relativistic mass of the electron is a function of its velocity and is greater than its rest mass.

$$\frac{h}{m\lambda} = \frac{h}{m_0\lambda_0} \sqrt{1 - \frac{v^2}{c^2}} \quad \text{or} \quad \lambda = \lambda_0 \sqrt{1 - \frac{v^2}{c^2}}$$

Let  $\lambda_0$  be the wavelength of the incident radiation. Then the wavelength of the scattered radiation is given by

$$\lambda = \lambda_0 \sqrt{1 - \frac{v^2}{c^2}}$$

For values of  $v$  less than

$v$	$\lambda$	$\lambda_0$	$\frac{\lambda}{\lambda_0}$
0	$\lambda_0$	$\lambda_0$	1
$\frac{c}{2}$	$\lambda_0 \sqrt{1 - \frac{1}{4}}$	$\lambda_0$	$\frac{\sqrt{3}}{2}$
$\frac{c}{\sqrt{2}}$	$\lambda_0 \sqrt{1 - \frac{1}{2}}$	$\lambda_0$	$\frac{1}{\sqrt{2}}$
$c$	0	$\lambda_0$	0

the value of  $v$  increases, the wavelength of the scattered radiation decreases. For values of  $v$  greater than  $\frac{c}{2}$ , the wavelength of the scattered radiation is less than the wavelength of the incident radiation.

$$\frac{h}{m\lambda} = \frac{h}{m_0\lambda_0} \sqrt{1 - \frac{v^2}{c^2}} \quad \text{or} \quad \lambda = \lambda_0 \sqrt{1 - \frac{v^2}{c^2}}$$

Let  $\lambda_0$  be the wavelength of the incident radiation. Then the wavelength of the scattered radiation is given by  $\lambda = \lambda_0 \sqrt{1 - \frac{v^2}{c^2}}$ . For values of  $v$  less than  $\frac{c}{2}$ , the wavelength of the scattered radiation is greater than the wavelength of the incident radiation. For values of  $v$  greater than  $\frac{c}{2}$ , the wavelength of the scattered radiation is less than the wavelength of the incident radiation.

In summary, the wavelength of the scattered radiation is a function of the velocity of the electron. For values of  $v$  less than  $\frac{c}{2}$ , the wavelength of the scattered radiation is greater than the wavelength of the incident radiation. For values of  $v$  greater than  $\frac{c}{2}$ , the wavelength of the scattered radiation is less than the wavelength of the incident radiation.

energy spread,  $\delta E$ , of the scattered protons. Heyens<sup>19</sup> points out that resonance scattering will be most readily detectable for small  $E$ , large scattering angles ( $\sim 180^\circ$ ) and for energies  $E$  for which the level width (strongly dependent on  $E$  due to barrier penetration) is comparable to the experimental resolution and yet not so large that discrete level structure disappears. It is also necessary to assume that there is no other process more probable than elastic scattering.

For proton energy,  $E_0 = 1$  Mev., scattering angle  $\theta = 150^\circ$ , using argon as the scattering nucleus,  $Z = 18$ , the ratio becomes:

$$\frac{\sigma_r}{\sigma_c} = 9.42 \left( \frac{\Gamma_r}{\delta E} \right)$$

In other words, if the energy resolution should be as much as five times the level width, the ratio of maximum resonance scattering to Coulomb scattering (neglecting other processes) would still be about two to one.

#### Bethe's Formula.

Bethe<sup>27</sup> derived an expression for the ratio of total scattering to Coulomb scattering near a single resonance which includes provision for total angular momentum and spin of the scattering nucleus and incident particle:

$$x = \frac{\sigma}{\sigma_c} = 1 + \frac{2J + 1}{(2I + 1)(2s + 1)} \cdot \frac{p^2 + 2p \sin \xi + 2p x \cos \xi}{(1 + x^2)}$$

The first part of the paper is devoted to a discussion of the  
 various methods which have been proposed for the determination of  
 the rate of reaction in the case of a reaction of the type  

$$A + B \rightarrow C + D$$
 in which the reactants are in the same phase. The methods  
 discussed are the method of initial rates, the method of  
 integrated rate laws, the method of half-lives, and the  
 method of isolation. The method of initial rates is the  
 simplest and most direct method, but it is only applicable  
 to reactions of the type  $A + B \rightarrow C + D$  in which the  
 reactants are in the same phase. The method of integrated  
 rate laws is applicable to reactions of the type  $A + B \rightarrow C + D$   
 in which the reactants are in the same phase, and the  
 method of half-lives is applicable to reactions of the type  

$$A \rightarrow B + C$$
 in which the reactant is in the same phase. The method of  
 isolation is applicable to reactions of the type  $A + B \rightarrow C + D$   
 in which the reactants are in the same phase, and the  
 rate of reaction is determined by measuring the rate of  
 disappearance of one of the reactants.

$$\left(\frac{7}{2}\right)^{0.66} = \frac{70}{20}$$

The second part of the paper is devoted to a discussion of the  
 various methods which have been proposed for the determination of  
 the rate of reaction in the case of a reaction of the type  

$$A + B \rightarrow C + D$$
 in which the reactants are in different phases. The methods  
 discussed are the method of initial rates, the method of  
 integrated rate laws, the method of half-lives, and the  
 method of isolation. The method of initial rates is the  
 simplest and most direct method, but it is only applicable  
 to reactions of the type  $A + B \rightarrow C + D$  in which the  
 reactants are in the same phase. The method of integrated  
 rate laws is applicable to reactions of the type  $A + B \rightarrow C + D$   
 in which the reactants are in the same phase, and the  
 method of half-lives is applicable to reactions of the type  

$$A \rightarrow B + C$$
 in which the reactant is in the same phase. The method of  
 isolation is applicable to reactions of the type  $A + B \rightarrow C + D$   
 in which the reactants are in the same phase, and the  
 rate of reaction is determined by measuring the rate of  
 disappearance of one of the reactants.

The third part of the paper is devoted to a discussion of the  
 various methods which have been proposed for the determination of  
 the rate of reaction in the case of a reaction of the type  

$$A + B \rightarrow C + D$$
 in which the reactants are in the same phase. The methods  
 discussed are the method of initial rates, the method of  
 integrated rate laws, the method of half-lives, and the  
 method of isolation. The method of initial rates is the  
 simplest and most direct method, but it is only applicable  
 to reactions of the type  $A + B \rightarrow C + D$  in which the  
 reactants are in the same phase. The method of integrated  
 rate laws is applicable to reactions of the type  $A + B \rightarrow C + D$   
 in which the reactants are in the same phase, and the  
 method of half-lives is applicable to reactions of the type  

$$A \rightarrow B + C$$
 in which the reactant is in the same phase. The method of  
 isolation is applicable to reactions of the type  $A + B \rightarrow C + D$   
 in which the reactants are in the same phase, and the  
 rate of reaction is determined by measuring the rate of  
 disappearance of one of the reactants.

$$\frac{2 \times 9 + 2 \times 2 + 2 \times 1}{2 \times 2} = \frac{2 \times 2 + 2 \times 1 + 2 \times 1}{2 \times 2} = 1$$

where:  $\sigma$  = total scattering cross-section per unit solid angle  
 $\sigma_c$  = Coulomb (Rutherford) scattering cross-section  
 $J$  = total angular quantum number of the compound nucleus  
 $i$  = spin of scattering nucleus  
 $s$  = spin of incident particle

$$x = \frac{2(E - E_r)}{\Gamma_r}$$

$E$  = energy of incident particle

$E_0$  = energy at resonance

$\Gamma_r$  = total level width

$$p = \frac{2\chi v}{e^2 z^2} \left[ \frac{\Gamma_{sp}^r}{\Gamma_r} \right] \sin^2\left(\frac{\theta}{2}\right)$$

$\Gamma_{sp}^r$  = partial width of resonance level (corresponding to emission of the incident particle  $P$  with the scattering nucleus being left in the ground state  $p$ )

$$\xi = \alpha \log \sin^2\left(\frac{\theta}{2}\right)$$

$\theta$  = scattering angle in center of mass coordinates

$$\alpha = \frac{zZe^2}{\chi v}$$

$v$  = velocity of incident particle

$Z$  = atomic number of scattering nucleus

$z$  = atomic number of incident particle

$$\chi = \frac{h}{2\pi} \quad (\text{Planck's constant})$$

Rose<sup>28</sup> puts the equation into slightly different form:

$$R = 1 + \frac{p^2 + 2 p \sin \xi + 2 p x \cos \xi}{1 + x^2}$$

$$\text{where } p = (2J + 1) \left( \frac{Z}{Y} \right) \left( \frac{\Gamma_{sp}}{\Gamma_r} \right) \sin^2\left(\frac{\theta}{2}\right) J(\cos \theta)$$

$$Y = \frac{zZe^2}{\chi v}$$

$$\xi = \alpha \log \sin^2\left(\frac{\theta}{2}\right)$$

1. The first step is to determine the initial conditions of the system. This involves identifying the state variables and their initial values at time  $t=0$ .

$$\begin{aligned}
 & \text{Initial conditions: } x(0) = x_0, \dot{x}(0) = \dot{x}_0 \\
 & \text{The system is described by the differential equation:} \\
 & m \ddot{x} + c \dot{x} + kx = F \cos(\omega t)
 \end{aligned}$$

where  $m$  is the mass,  $c$  is the damping coefficient,  $k$  is the spring constant, and  $F$  is the amplitude of the external force.

$$\text{The steady-state response is given by: } x_{ss}(t) = \frac{F}{\sqrt{(k - m\omega^2)^2 + c^2\omega^2}} \cos(\omega t - \phi)$$

where  $\phi$  is the phase shift between the response and the excitation. The phase shift is determined by the frequency ratio  $r = \omega/\omega_n$  and the damping ratio  $\zeta$ .

$$\phi = \tan^{-1} \left( \frac{c\omega}{k - m\omega^2} \right)$$

The resonance frequency  $\omega_n$  is the frequency at which the system exhibits maximum response.

$$\omega_n = \sqrt{\frac{k}{m}}$$

The damping ratio  $\zeta$  is a dimensionless parameter that indicates the level of damping in the system.

It is defined as the ratio of the actual damping coefficient to the critical damping coefficient.

$$\zeta = \frac{c}{2\sqrt{km}}$$

$$\text{The magnification factor } Q \text{ is defined as the ratio of the steady-state amplitude to the static deflection:}$$

$$Q = \frac{1}{2\zeta\sqrt{1 - \zeta^2}}$$

$P_J(\cos \Theta) =$  Legendre polynomial of order  $J$

$$e^{i\delta} = e^{i\delta_0} \prod_{l=1}^J \frac{(n + i\gamma)^2}{n^2 + \gamma^2}$$

If we assume that the only energetically possible process other than scattering of the incident particle is gamma emission and since radiation widths are negligible compared to particle widths, especially for light nuclei, for all practical purposes we may take,

$$\frac{\Gamma_{pp}^r}{\Gamma_r} = 1$$

With this assumption the constants for Bethe's ratio have been computed for the particular experimental arrangement used for the present problem of scattering of protons from argon at an angle of  $150^\circ$ , assuming  $l = 0$  and  $s = \frac{1}{2}$  (reference 24),

$$R = \frac{\sigma}{\sigma_0} = 1 + 0.324 (2J + 1) (0.260 + 1.962 x) / (1 + x^2)$$

If we assume  $\Gamma_r = 50$  Kev., then  $x = 40(E - E_0)$ . Using this value and  $J = 0$ , the above ratio is plotted in Fig. 4. This curve shows the general shape of an anomaly in the Rutherford scattering. Naturally, this anomaly will be superimposed on the Rutherford scattering curve which is plotted in Fig. 3 for arbitrary units along the ordinate using 100 at an energy of 1 Mev. It will be noted that an increase in  $J$  (higher angular momentum quantum number of

$$\frac{L}{L_0} = \frac{1}{1 + \alpha^2}$$

It is known that the ratio  $\frac{L}{L_0}$  is a function of the parameter  $\alpha$  and is determined by the expression  $\frac{L}{L_0} = \frac{1}{1 + \alpha^2}$ . The ratio  $\frac{L}{L_0}$  is a function of the parameter  $\alpha$  and is determined by the expression  $\frac{L}{L_0} = \frac{1}{1 + \alpha^2}$ . The ratio  $\frac{L}{L_0}$  is a function of the parameter  $\alpha$  and is determined by the expression  $\frac{L}{L_0} = \frac{1}{1 + \alpha^2}$ .

$$\frac{L}{L_0} = \frac{1}{1 + \alpha^2}$$

Fig. 3. Dependence of the ratio  $\frac{L}{L_0}$  on the parameter  $\alpha$ . The ratio  $\frac{L}{L_0}$  is a function of the parameter  $\alpha$  and is determined by the expression  $\frac{L}{L_0} = \frac{1}{1 + \alpha^2}$ . The ratio  $\frac{L}{L_0}$  is a function of the parameter  $\alpha$  and is determined by the expression  $\frac{L}{L_0} = \frac{1}{1 + \alpha^2}$ . The ratio  $\frac{L}{L_0}$  is a function of the parameter  $\alpha$  and is determined by the expression  $\frac{L}{L_0} = \frac{1}{1 + \alpha^2}$ .

The ratio  $\frac{L}{L_0}$  is a function of the parameter  $\alpha$  and is determined by the expression  $\frac{L}{L_0} = \frac{1}{1 + \alpha^2}$ . The ratio  $\frac{L}{L_0}$  is a function of the parameter  $\alpha$  and is determined by the expression  $\frac{L}{L_0} = \frac{1}{1 + \alpha^2}$ . The ratio  $\frac{L}{L_0}$  is a function of the parameter  $\alpha$  and is determined by the expression  $\frac{L}{L_0} = \frac{1}{1 + \alpha^2}$ . The ratio  $\frac{L}{L_0}$  is a function of the parameter  $\alpha$  and is determined by the expression  $\frac{L}{L_0} = \frac{1}{1 + \alpha^2}$ .



Ratio of Total to Coulomb Scattering near a Resonance (Ang. momentum,  $J=0$ )

Assuming  $\Gamma_r = 50 \text{ Kev.}$

Lab. Angle =  $150^\circ$

$$\frac{\sigma}{\sigma_c} = 1 + 0.324(0.260 + 1.962 \chi) / (1 + \chi^2)$$

$$\chi = \frac{2(E - E_0)}{\Gamma_r}$$

Reference:  
Bethe. Rev. Mod. Phys. 2, 69 (1937)

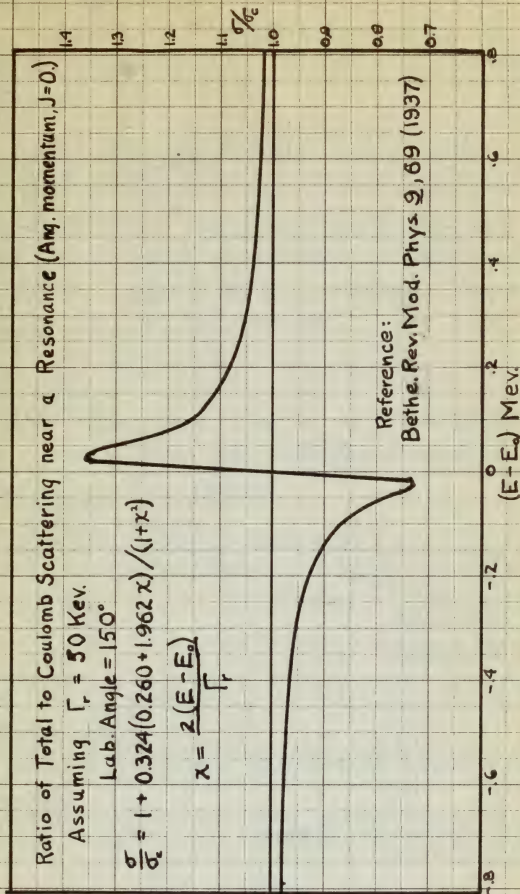


FIGURE 4.



compound nucleus) serves to increase the magnitude of both the positive peak and the negative peak, but does not change the spread between the peaks. In other words, the anomaly is sharpened.

The plot of  $\frac{1}{\sin^4(\frac{\theta}{2})}$  in Fig. 8 shows the strong dependence of Rutherford scattering on angle and consequently the advantage of using an angle near  $180^\circ$ . It will be noted that at an angle of  $90^\circ$  the scattering is almost four times that at  $150^\circ$ , whereas at the latter angle it is only 1.15 times the true back scatter at  $180^\circ$ .

### Level Widths.

Rose<sup>28</sup> also gives a method for estimating the level width from experimental data. The maximum and minimum scattering ratios are given by:

$$R_{1,2} = 1 + \frac{1}{R} \frac{\Gamma(E_{1,2}) b}{E_{1,2} - E_0} \quad \text{where } b = 2 \rho \cos \xi$$

$E_0$  = resonance energy  
 $E_{1,2}$  = energy values at maximum and minimum values of R  
 $R_{1,2}$  = maximum and minimum values of R

Since the only unknown is  $\Gamma$ , the level width can be found from this formula.

Also the level width without Coulomb barrier may be found from:

$$\Gamma_x = \frac{G}{\Gamma} P \quad \text{where } G_x = \text{level width without Coulomb barrier}$$



$P$  is the penetrability calculated from well known formulae by Bethe<sup>27</sup>. Rose also gives a simple method of determining  $J$  if interference scattering is neglected at the extrema of the anomaly. The extrema are also given by:

$$R_{1,2} = 1 + \frac{b}{2x_{1,2}} \quad \text{and} \quad x_{1,2} = -\frac{a}{b} \pm \left(1 + \frac{a^2}{b^2}\right)^{1/2}$$

combining,

$$\begin{aligned} \text{where } a &= c^2 + 2P \sin \zeta \\ b &= 2P \cos \zeta \end{aligned}$$

$$P = \frac{1}{2} (R_1^{1/2} - R_2^{1/2})$$

and since  $P$  is also given by definition to be:

$$P = (2J + 1) \left(\frac{Z}{r}\right) \left(\frac{\int_r^r}{\int_r}\right) \sin^2 \left(\frac{\theta}{2}\right) P_J(\cos \theta)$$

$$\text{where } \gamma = \frac{Zec^2}{\hbar v}$$

the only unknown parameter is  $J$ .

Resonance energy always lies between the extrema. The maximum error therefore in taking it to lie midway between would be one-half the separation between extrema or about one-fourth of the level width. The effect of straggling, i.e., beam spread in energy through the target, in shifting the higher extremum toward higher energies and lower energy extremum toward lower energies, thus increasing their separation by about the straggling width, increases the uncertainty in the resonance energy by a like amount.

It is the responsibility of the...  
 The...  
 The...  
 The...

$$\frac{1}{2} \left( \frac{1}{2} + \frac{1}{2} \right) = \frac{1}{2}$$

$$\frac{1}{2} \left( \frac{1}{2} + \frac{1}{2} \right) = \frac{1}{2}$$

$$\frac{1}{2} \left( \frac{1}{2} + \frac{1}{2} \right) = \frac{1}{2}$$

and more 6 is also given by definition so that

$$\frac{1}{2} \left( \frac{1}{2} + \frac{1}{2} \right) = \frac{1}{2}$$

$$\text{where } \gamma = \frac{1}{2}$$

The... is...

The... is...

The... is...

The... is...

The... is...

The... is...

The... is...

The... is...

The... is...

The... is...

The... is...

### Recent Experiments.

Two groups at the University of Wisconsin have recently demonstrated the power of using elastic scattering to investigate excited levels in light nuclei.

Bender, Shoemaker, Kaufmann, and Bouricinus<sup>29</sup> have investigated the 985. Kev. resonance in  $Al^{27}$  by means of the elastic scattering of protons. The variation in scattering yield is in very good agreement with the above theory near the resonance. Elastic scattering of protons from  $Mg^{24}$  was investigated throughout a range of proton energy from 0.40 to 3.95 Mev. by Mooring, Koester, Goldberg, Saxon, and Kaufmann.<sup>30</sup> Anomalies of varying shapes other than the type shown in Fig. 4 were discovered. The general discussion of the theory of such anomalies has been made by Leubenstein and Leubenstein<sup>31</sup>. This theory includes not only the interference caused by phase shifts induced by energy levels of the compound nucleus but also that due to the hard sphere type of scattering. A vector method of analysis of anomalies is given which enables one to calculate the shape of anomalies based on an assumption of the total angular momentum of the compound nucleus. The predicted shapes for the various arbitrary values of  $J$  chosen can be compared with the curves from experimental data. The "best fit" then can be assumed to yield the correct value of  $J$ .

In a later article Koester<sup>32</sup> gives a fairly complete





analysis of the resonances found in  $Mg^{24}$  by Hoerling, Koester, et al. along the line of the theory just mentioned. He points out that the parity  $P$  of the excited nucleus is related to the parity  $p$  of the ground state of the target nucleus by the expression,

$$P = (-1)^L p$$

where  $L$  is the orbital angular momentum value of the incident proton with spin value  $\frac{1}{2}$ . The value of  $L$  is given by,

$$J = L \pm \frac{1}{2}$$

for target nuclei of spin zero. Since the qualitative shape of a resonance anomaly depends strongly on particular values of  $J$  and  $L$ , the angular momentum and parity number of energy levels can be determined.

Since  $A^{40}$  is a nucleus of zero spin, it satisfies the requirements of the above theory.

We have seen that the following information can be obtained from an analysis of anomalies in elastic scattering of protons on nuclei of spin zero:

- (a) Energy levels of excited states of the compound nucleus,
- (b) Angular momentum of excited states of the compound nucleus,
- (c) Relative parity numbers of the excited states,
- (d) Level widths of the resonances, and
- (e) Level widths without Coulomb barrier.

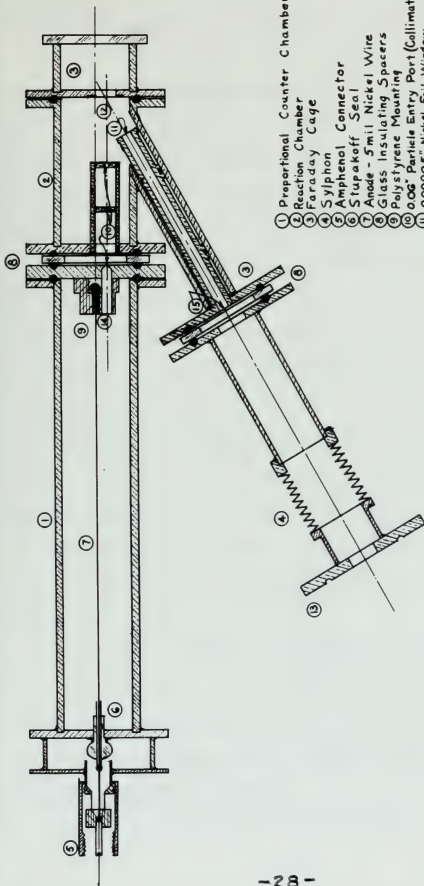


#### IV. APPARATUS: DESCRIPTION, CALIBRATION, BASIC CALCULATIONS

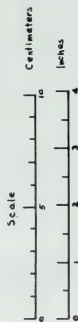
##### Mechanical Parts.

The apparatus originally designed by Commander A. B. Chilton<sup>33</sup>, U.S. Navy, during his graduate work at The Ohio State University is shown in Fig. 6. It consists of five principal parts: (1) a connecting piece which attaches to the end of the proton tube in the magnetic analysing section of the Van de Graaff generator; (2) the beam collimator which restricts the proton beam to a diameter of 0.1" and directs it into the reaction chamber; (3) the reaction chamber which serves also as a Faraday cage, in which the proton reaction occurs and the ion current is collected after passing through a nickel foil window; (4) the reaction collimator consisting of three collinear ports, 0.06" in diameter, aligned at a laboratory angle of  $150^\circ$  from the proton beam, and which serves to define the target area and to align the scattered particles entering the detection chamber; and (5) the counter itself, which is a typical gas-filled proportional counter collecting ionization pulses from the collimated beam of reaction or scattered particles entering via the reaction collimator. The last of the three small 0.06" ports in the reaction collimator is mechanically integral with the proportional counter, being in the end wall of the sensitive chamber.





Note: Gas Filling Parts Not Shown.

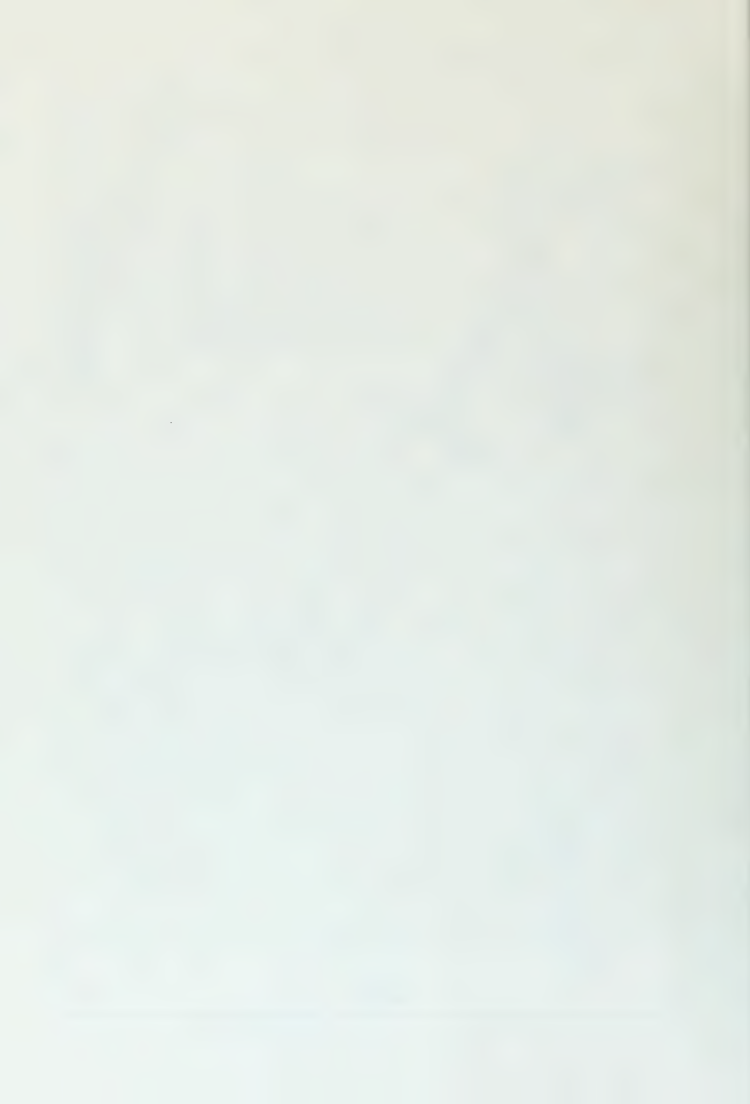


## PROTON REACTION DETECTOR

### Mechanical Details

Designed by: A.B.Chilton, May 1951.  
 Modified by: J.O.F.Dorsett, March 1952.

FIGURE 5.



This end wall of the counter also serves as an electrostatic shield between the Faraday cage and sensitive volume.

Certain modifications have been made in the original design. These include: (1) glass insulating rings substituted for lucite; (2) except for the entry port, completely enclosing the sensitive volume with brass to avoid spurious counts due to a capacity which formerly existed between the floating end of the central wire and the Faraday cage; (3) addition of the reaction collimator and modification of the proton beam collimator; (4) changing all internal valves to the bellows type needle valve.

The reaction collimator serves to limit the extent of the proton beam from which the scattered protons are being counted. The geometry of the apparatus is such that the extreme thickness of the gaseous target under surveillance is about 1.3 centimeter. Since the argon is under a reduced pressure of 75 mm.  $Hg$ , the equivalent thickness at standard pressure is about 1 mm.

The counting chamber is operated in the proportional region. It is fitted with a gas manifold providing connections to gas tanks, vacuum pump, and mercury manometer. Multiple connections allow mixtures to be used and permit flexibility of pressure control.

A nickel foil window, 0.05 mil thick at the end of the

This was well at the meeting time arrived as in class.

-

1999

and return to the bottom type media wire.

into it about a mile.

[illegible]



beam collimator provides a vacuum seal between the reaction chamber and the Van de Graeff vacuum system. This foil is designed to withstand a pressure of one atmosphere against the outer side; but in actual operation no more than 250 mm. Hg is ever necessary since a vacuum cross connection permits simultaneous evacuation of all parts of the apparatus. After the vacuum is obtained, the valve in the cross connection can be closed thus isolating the manifold and counting chamber from the Van de Graeff vacuum system.

The central wire of the proportional counter is a 5 mil nickel wire supported at the free end in a glass capillary bulb enclosed in a polystyrene mounting. The other end passes through a Stupakoff seal and thence to an amphenol connector which attaches directly to the preamplifier.

### Electronic Apparatus

The preamplifier is an Atomic Instrument Co. Preamplifier 205-B, originally built to be used with an ionization chamber with a time constant of 2.7 milliseconds. The time constant has been changed to 7.5 microseconds to make it appropriate for use with a proportional counter at fast counting rates. This instrument has two stages of amplification and two cathode followers incorporating inverse feedback to achieve a high order of gain stability. Pulse amplification is fixed at approximately 20. A special high voltage coaxial cable was built to allow voltages up to 1200 volts to be impressed on the central wire of the proportional

beam splitter system is shown in Figure 1. The beam splitter is a thin film of silver on glass. The light is incident on the beam splitter at an angle of 45 degrees. The light is split into two beams. One beam is reflected and the other is transmitted. The reflected beam is focused by a lens and the transmitted beam is focused by another lens. The two beams are then recombined by a second beam splitter. The resulting beam is then focused by a lens and the light is detected by a photodiode.

Experimental Results

The experimental results are shown in Figure 2. The results show that the beam splitter system is capable of splitting the light into two beams. The reflected beam is focused by a lens and the transmitted beam is focused by another lens. The two beams are then recombined by a second beam splitter. The resulting beam is then focused by a lens and the light is detected by a photodiode.

counter. Filament and plate voltages are supplied by a Model 204-B amplifier built by Atomic Instrument Co.

The output from the pre-amplifier is fed to the Model 204-B Linear Amplifier. The gain from this instrument is not too essential when used with the 206-B Pre-amplifier; the amplifier is used as a pulse shaper and discriminator. A pulse amplitude discriminator passes all pulses received above that voltage set on the discriminator dial. Linearity of dial setting is better than 2% from 0 to 100 volts. Three different rise times are provided: 5, 0.8, and 0.2 microseconds with decay times of about 25 , 4 , and 0.4 microseconds. Output from the discriminator is a constant 10 volt, 0.4 microsecond pulse which is fed to a Model 1030 Atomic Instrument Co. Scaler. An oscilloscope is operated from the high level output of the amplifier.

High voltage power for the central wire of the proportional counter is obtained from a Model 1090, 5000 volt Regulated Power Supply built by Nuclear Instrument and Chemical Corporation. This power source can supply either positive or negative voltage from zero to maximum value with regulation to within 0.02% of output voltage.

A sensitive integrator is connected to the Murray cage to determine the total proton ion charge collected. This instrument was designed and built by W. E. L. Boyce<sup>54</sup> during his graduate work at The Ohio State University in 1958-1959.

[illegible]

The integration is accomplished by collection of positive charge on a special polystyrene condenser having a capacity of 0.982 microfarad, which is charged to a negative potential of about 10 volts, the exact value must be measured at the charging battery. The integrator has a controlling relay which operates the scaler so that it registers only during the integration period. The instrument may be set to operate for several different specified cycles of charge and discharge of the integrating condenser from one cycle to 24 cycles of operation, depending on the intensity of the proton beam. One cycle of the integrator will be equivalent to a charge given by the following expression:

$$Q = CV = 0.982V \quad \text{where } V = \text{battery voltage} \\ \text{in microcoulombs}$$

If the battery is exactly 10 volts, the charge will be 9.82 microcoulombs which is equivalent to  $6.13 \times 10^{13}$  protons. The design was such that one cycle would be approximately equivalent to collection of 10 microcoulombs or  $6.24 \times 10^{13}$  protons. A counting period of ten seconds would therefore mean a beam current of 1 microampere. The error of the integrator for ion currents greater than 0.06 microampere due to leakage is less than  $\pm 1\%$ . For charging voltages of about 10 volts the error in collected charge due to leakage is therefore less than  $\pm 0.1\%$ . For runs of length greater than 10 seconds (i.e. currents less than 1 microampere) the error due to relay time is less than 0.5%.

The investigation is continuing at Washington DC and it is expected that a report will be made available by the end of the year.

have only taken the information coming. The informant  
visited today which revealed the matter as that is really  
connected to the shipping history. The informant has a son

may be met as follows: The various different quantities  
of change and change of the following quantities  
are from the point of view of the following quantities  
the following of the following quantities. The following  
will be a list of the following quantities.

[illegible]

Two to leakage is therefore less than  $\frac{1}{2}$  G.P. For each of



The integrator appears to be dependable to within  $\pm 1\%$  for ion beam currents of 0.06 to 1 microampere.

The electronic and gas filling systems are shown in Fig. 6. A positive potential of +90 volts is maintained on the insulated connecting piece to prevent secondary electrons scattered from the first port of the beam collimator from being collected in the Faraday cage and thus giving an erroneous integration of beam current.

### Calibration.

The proton energy resolution is determined by a 1 mm. slit 70 cm. from the center of the magnet pole faces. The beam at this point has been deflected through an angle of  $30^\circ$  from the neutral beam axis of the Van de Graaff. The resolution is calculated as follows:

Let  $L$  = length of magnet pole face  
 $r$  = radius of arc along which the beam is deflected between magnet pole faces.  
 $A$  = angle through which beam is deflected.

Then,  $L = r \sin A$

$$\frac{dr}{r} = -\cot A \, dA$$

$$dA = 0.1 \text{ cm} / 70 \text{ cm.} = 1.43 \times 10^{-3}$$

Therefore,  $dr/r = -2.48 \times 10^{-3}$

Neglecting the variation of the magnet current,  $dr/r$  is approximately equal to  $dE/2E$  since  $r$  is proportional to  $\sqrt{E}$ .

Using this approximation,

$$dE/E = 0.5\%$$

The following table is a summary of the data obtained from the experiments. The data are given in the form of a table, and the results are discussed in the text. The data are given in the form of a table, and the results are discussed in the text. The data are given in the form of a table, and the results are discussed in the text.

# Discussion

The results of the experiments are discussed in this section. The data are given in the form of a table, and the results are discussed in the text. The data are given in the form of a table, and the results are discussed in the text. The data are given in the form of a table, and the results are discussed in the text.

The data are given in the form of a table, and the results are discussed in the text. The data are given in the form of a table, and the results are discussed in the text. The data are given in the form of a table, and the results are discussed in the text.

$$A = 0.1 \text{ cm} \times 10^{-8}$$

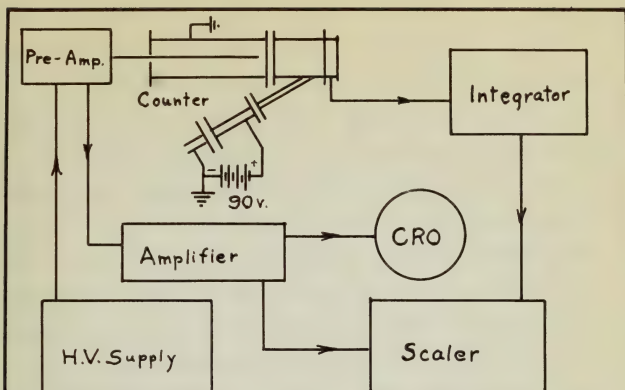
$$A = 0.1 \text{ cm} \times 10^{-8}$$

Therefore, the variation of the magnetic field is given by the following equation:

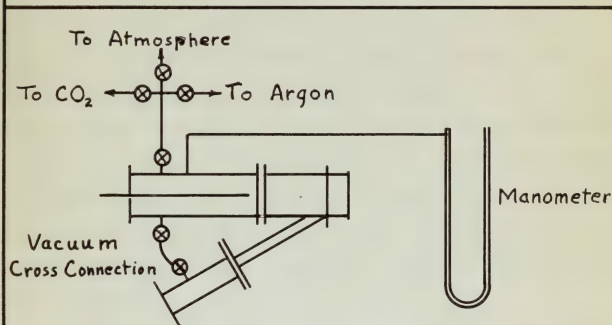
$$B = 0.1 \text{ cm} \times 10^{-8}$$

The results of the experiments are discussed in this section. The data are given in the form of a table, and the results are discussed in the text. The data are given in the form of a table, and the results are discussed in the text.





## ELECTRICAL CONNECTIONS



## GAS AND VACUUM CONNECTIONS

FIGURE 6.



or at an energy of 1 Mev.,  $dE \approx 5$  kev.

The magnet was calibrated for this slit setting on the 0.873 Mev. gamma resonance of  $P^{19}$  using a LiF target.

Amplification factors for the gas amplification in the proportional counter were obtained by using an internal source of alphas consisting of a thin layer of polonium salt evaporated on a tantalum disc. This was inserted in the target mounting. The counter was filled with various pressures and at each one the central wire voltage was varied. Pulse sizes were determined by observation on an oscilloscope. In actual practice, the pulse size was maintained constant on the screen of the oscilloscope by varying the gain on the linear amplifier. The reference point was taken as that gain necessary to produce the pulse height with the counter voltage so low that amplification was essentially unity, i.e., when the counter was operating in the ionization chamber region. Reciprocals of gain settings for a given constant pressure then became the relative amplification factors of the counter tube assuming the gain setting for the ionization region represented an amplification of unity. Curves of amplification factors are plotted in Figure 7.

A discriminator curve was run on the internal  $Po^{210}$  source. Data are given in Table I, and the curve is plotted in Figure 8.

as an example of a new...

The present work... the first...

...the first...

...the first...

...the first...

...the first...

...the first...

...the first...

...the first...

...the first...

...the first...

...the first...

...the first...

...the first...

...the first...

...the first...

...the first...

...the first...

...the first...

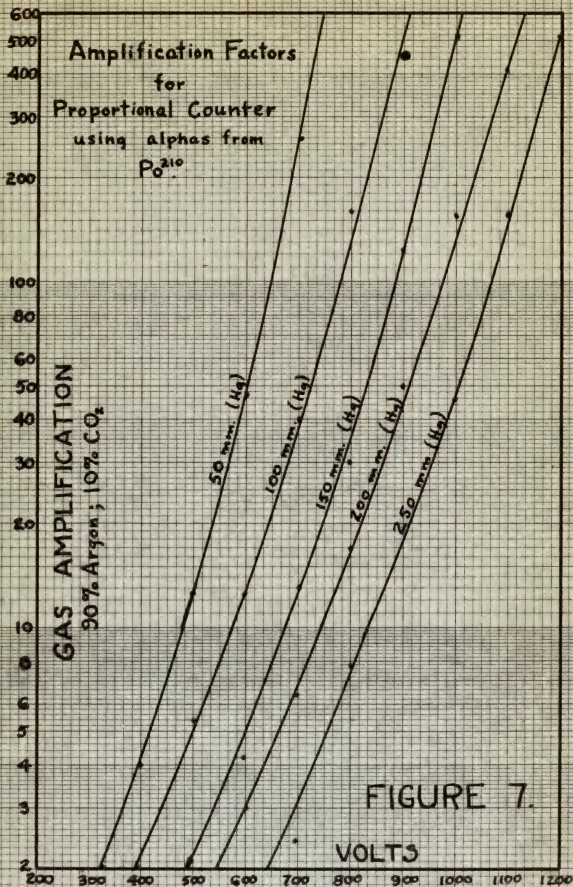
...the first...

...the first...

...the first...

...the first...

...the first...





# Discriminator Curve on Internal Target - $Po^{210}$

Alpha Counts/min. vs. Bias Voltage.

Pressure - 200 mm. Hg; 90% A, 10%  $CO_2$

Anode Voltage - +800 volts.

Using Model 205-B Preamplifier

Amplifier Gain, 2.

Rise Time, 0.2  $\mu s$ .

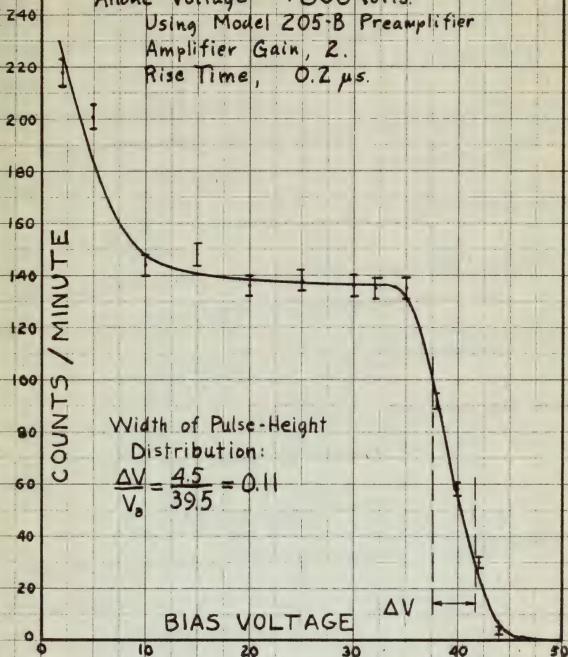


FIGURE 8.







Since the target for scattering from argon is a gaseous target, it was necessary to resort to actual measurements of the geometry of the reaction volume to determine the target thickness from which the energy spread in the target was computed. Similarly, the distances from target volume to sensitive volume of the counter were measured. These distances are recorded in Table II along with other experimental measurements.

The solid angle at the reaction subtended by the 0.06" entry port at the counter wall was computed to be:

$$\Delta\Omega_0 = \frac{1}{3144} \text{ steradian for the mean distance of 7.55 cm.}$$

from target to entry port. Since the entry port has a diameter of 0.06" or 0.152 cm. the computation is:

$$\Delta\Omega_0 = \frac{(0.152)^2 \pi}{4 \times (7.55)^2} = \frac{1}{3144} \text{ steradian.}$$

From the geometry of the reaction collimator the parallax subtended by the target is computed to be:

$$\Delta\theta_1 = \frac{0.152}{2.3} = 0.0663 \text{ radian}$$

The variation in scattering angle (laboratory system) is therefore,

$$\frac{\Delta\theta_1}{2} = \Delta\theta_0 = \pm 1.9^\circ$$



The laboratory scattering angle is then,

$$\Theta = 150^\circ \pm 1.9^\circ.$$

### Basic Calculations.

The conversion of scattering angle from the laboratory system to the center of mass system is accomplished by the relation,

$$\Theta_{cm} = \Theta + \arcsin \left[ \frac{M}{M_A} \sin \Theta \right]$$

where  $\Theta_{cm}$  = scattering angle, center of mass

$\Theta$  = scattering angle, laboratory

$M_P$  = mass of proton

$M_A$  = mass of scattering nucleus

Substituting values for mass of argon nucleus and laboratory angle,

$$\Theta_{cm} = 2.6180 + \arcsin \left[ \frac{1}{40} \times 0.5 \right] = 2.6180 + 0.0125 \text{ (radians)}$$

$$\begin{aligned} \Theta_{cm} &= 2.6305 \text{ (radians)} \\ &= 151^\circ 45.1' \end{aligned}$$

The reduced mass of the proton for elastic collision with an argon nucleus is:

$$\begin{aligned} \mu &= \frac{M_P M_A}{M_P + M_A} = \frac{40.08}{45.95} = 0.893 \text{ amu} \\ &= 1.642 \times 10^{-24} \text{ gram.} \end{aligned}$$

Energy conversion from the laboratory system to the center-of-mass system is given by:

The laboratory concerning angle is then,

$$\theta = 180^\circ \pm 1.0^\circ$$

### Angle of Incidence

The angle of incidence is the angle between the incident ray and the normal to the surface of the crystal. It is denoted by  $\theta_i$ .

$$\theta_i = \theta_r + \theta_t$$

- $\theta_i$  = angle of incidence
- $\theta_r$  = angle of reflection
- $\theta_t$  = angle of refraction

For a given angle of incidence, the angle of reflection is equal to the angle of incidence.

$$\theta_i = \theta_r + \theta_t = 180^\circ - \theta_t + \theta_t = 180^\circ$$

$$\theta_i = 180^\circ$$

The angle of incidence is the angle between the incident ray and the normal to the surface of the crystal. It is denoted by  $\theta_i$ .

$$\theta_i = \theta_r + \theta_t = 180^\circ - \theta_t + \theta_t = 180^\circ$$

For a given angle of incidence, the angle of reflection is equal to the angle of incidence.

$$E = E_0 \left[ \frac{M_A}{M_A + M_P} \right] = \frac{32.94}{40.95} E_0$$

$$E = 0.975 E_0$$

In order to determine what the energy of the proton is at the scattering nucleus, it is necessary to calculate the loss in energy of the beam while passing through the nickel window and the filling gas between the window and reaction volume.

Chilton<sup>33</sup> has computed the energy thickness of the 0.00006" nickel foil window for various energies of protons. The energy of the beam minus this value is the net energy available in the reaction chamber at the window. This has been plotted as Curve I in Figure 10.

In computing the loss in energy due to passage through the filling gas, we make use of the range tables for pure argon based on experimental and theoretical considerations by Hirschfelder and Magee<sup>35</sup>. These data were plotted as a range curve in Figure 9. The presence of 10% CO<sub>2</sub> is not considered to effect the correctness of the calculations owing to the uncertainties of the basic data and the inaccuracies of measurement of the dimensions of the apparatus.

Furthermore, the presence of 10% CO<sub>2</sub> is not considered

$$x = \frac{\left[ \frac{A}{B} + \frac{C}{D} \right]}{\left[ \frac{A}{B} + \frac{C}{D} \right]}$$

$$x = 0.078 R_0$$

In order to determine what the weight of the system is at the maximum weight, it is necessary to calculate the limit of the system of the system which is the system of the system and the system of the system and the system of the system.

Figure 1 shows the system of the system of the system.

Figure 1 shows the system of the system of the system. The system of the system of the system is the system of the system of the system. The system of the system of the system is the system of the system of the system.

In order to determine the system of the system of the system, the system of the system of the system is the system of the system of the system. The system of the system of the system is the system of the system of the system. The system of the system of the system is the system of the system of the system.

Figure 1

Figure 1 shows the system of the system of the system. The system of the system of the system is the system of the system of the system. The system of the system of the system is the system of the system of the system.

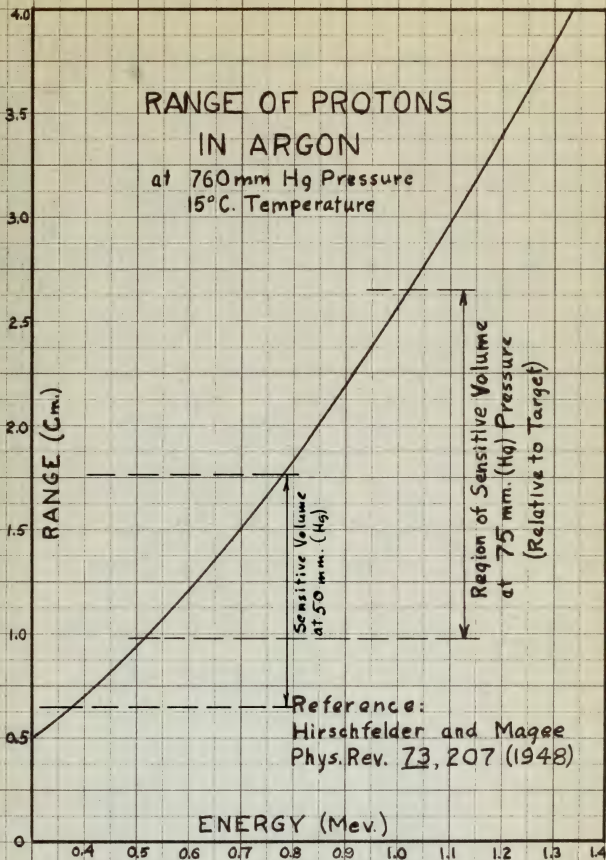
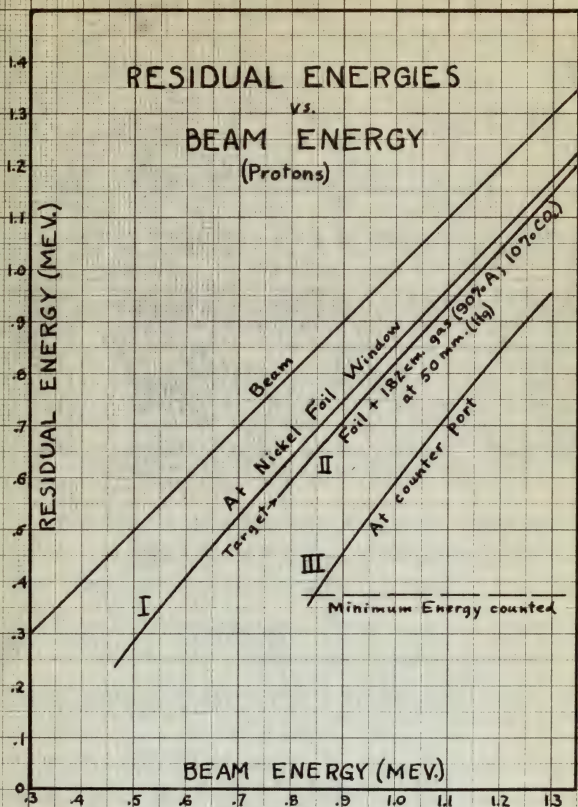


FIGURE 9.







**FIGURE 10.**



to have any appreciable effect on the intensity of Coulomb scattering inasmuch as the cross-section for this type of scattering is proportional to the fourth power of  $Z$ . The average  $Z$  for  $\text{CO}_2$  is 7.3 while for  $\text{A}$  it is 10. The ratio of cross-section due to argon to that due to  $\text{CO}_2$  (based on 90%  $\text{A}$ , 10%  $\text{CO}_2$ ) is:

$$\frac{\sigma_{\text{A}}}{\sigma_{\text{CO}_2}} = \frac{10^4 \times 0.9}{7.3^4 \times 0.1} = \frac{9.45 \times 10^4}{187} = 500$$

In other words the maximum error in neglecting the 10%  $\text{CO}_2$  is about 0.2%.

We may proceed to a calculation of the energy losses in the various portions of the reaction and counting chambers using the experimental measurements and the range curve for argon. The filling gas is at a pressure of 75 mm. Hg so all range measurements must be reduced by the factor, 75/760.

Table III is a computation of residual ranges and corresponding energies in argon at the extremities of the reaction volume for various initial beam energies. The difference between these energies is the spread in energy of elastically scattered protons due to thickness of the gaseous target. It is one factor in the experimental resolution.

Table IV is a computation of residual ranges and corresponding energies of elastically scattered protons upon reaching the sensitive volume of the counter. The spread

as there are considerable errors in the intensity of the  
 scattering measured in the present case. The  
 scattering is proportional to the square of the  
 average of the  $\alpha$  values. The  $\alpha$  values are  
 measured in the present case in the  $\alpha$  region.

$$\alpha = \frac{1}{2} \left( \frac{1}{\alpha_1} + \frac{1}{\alpha_2} \right) = \frac{1}{2} \left( \frac{1}{0.15} + \frac{1}{0.15} \right) = 0.15$$

In this case the average value is calculated as 0.15  
 in about 0.15.

The average value is calculated as 0.15 in the  
 present case. The average value is calculated as 0.15  
 in the present case. The average value is calculated as 0.15  
 in the present case.

The average value is calculated as 0.15 in the  
 present case. The average value is calculated as 0.15  
 in the present case. The average value is calculated as 0.15  
 in the present case.

The average value is calculated as 0.15 in the  
 present case. The average value is calculated as 0.15  
 in the present case. The average value is calculated as 0.15  
 in the present case.

The average value is calculated as 0.15 in the  
 present case. The average value is calculated as 0.15  
 in the present case. The average value is calculated as 0.15  
 in the present case.

The average value is calculated as 0.15 in the  
 present case. The average value is calculated as 0.15  
 in the present case. The average value is calculated as 0.15  
 in the present case.

The average value is calculated as 0.15 in the  
 present case. The average value is calculated as 0.15  
 in the present case. The average value is calculated as 0.15  
 in the present case.

in these energies is a measure of the difference in pulse sizes produced by the proportional counter. It will be noted that a large spread in these energies will give an apparent increase in counting rate as energy is increased above the threshold energy for counting, contrary to the theoretical reciprocal relation of Coulomb scattering to energy squared (Figure 3.) That is, the counting rate will increase until the entire spread of elastically scattered protons are entering the proportional counter. This occurs when the scattered proton has an energy (laboratory system) of about 535 kev. This value is arrived at by taking the distance from target to counter (see Fig. 9) which is the range of the minimum energy which can just reach the counter or 515 kev. and adding the straggling of 20 kev.

#### Sample Computation for Table III.

Beam energy	1 Mev.	Range	2.86 cm.
Loss in Ni window	-0.145 Mev.		
E at internal face of Ni	0.855	Range	2.03 cm.

Distance to reaction volume:

Minimum	1.50 cm.	Equivalent Range	0.128cm.
Maximum	2.33	"	0.230

Residual ranges of elastically protons:

Maximum, 2.03 - 0.128 = 1.90 cm.	Energy,	0.820 Mev.
Minimum, 2.03 - 0.230 = 1.80 cm.	"	0.792 "

Energy thickness of target,	0.028 Mev.
Average energy of elastically scattered protons,	0.806 "



### Sample Computation for Table IV.

Reaction ranges and energies:

Maximum

R  
1.90 cm.

E  
0.820 Mev.

Minimum

1.80 cm.

0.792 "

Distances to sensitive volume:

Maximum 10.4 cm.

Equivalent ranges:

Minimum 9.4 cm.

1.028 cm.

0.929 cm.

Residual ranges and energies in counter: R

Maximum (1.90 - 0.929)

0.97 cm.

E  
0.813 Mev.

Minimum (1.80 - 1.028)

0.77 cm.

0.427 "

Spread in range,

0.20 cm.

Spread in energy,

0.086 Mev.

Average energy of counted protons,

0.470 "

Spread in actual distance travelled in counter, 2.13 cm.

This is the worst possible condition and not the most probable. To arrive at the most probable spread in energies and therefore pulse sizes and energy resolution, we may treat the subject completely as a straggling problem.

### Straggling.

No account has so far been taken of straggling in the nickel foil or in the filling gas, or of beam resolution due to slit width.

Straggling in the nickel foil and argon gas has been treated as far as present theory permits by Chilton<sup>33</sup> who has computed the straggling for the particular case from a formula credited to Madsen and Venkateswarlu<sup>36</sup>.

$$\Omega^2 = \frac{4 Z^2 e^4}{M} \cdot \frac{Z_0 t}{\lambda}$$



# Single Component Ion Data

Ion	Concentration (M)	Activity (M)
H <sup>+</sup>	0.001	0.001
OH <sup>-</sup>	0.001	0.001

Concentration (M)	Activity (M)
0.001	0.001
0.001	0.001

Concentration (M)	Activity (M)
0.001	0.001
0.001	0.001

Concentration (M)	Activity (M)
0.001	0.001
0.001	0.001

It is noted that the activity of the ions is not equal to the concentration of the ions. This is due to the fact that the ions are not ideal and their activity is less than their concentration. The activity of the ions is given by the following equation:

$$a_i = \gamma_i \cdot c_i$$

where  $a_i$  is the activity of the ion,  $\gamma_i$  is the activity coefficient, and  $c_i$  is the concentration of the ion.

## Discussion

It is noted that the activity of the ions is not equal to the concentration of the ions. This is due to the fact that the ions are not ideal and their activity is less than their concentration. The activity of the ions is given by the following equation:

$$a_i = \gamma_i \cdot c_i$$

where  $a_i$  is the activity of the ion,  $\gamma_i$  is the activity coefficient, and  $c_i$  is the concentration of the ion.

It is noted that the activity of the ions is not equal to the concentration of the ions. This is due to the fact that the ions are not ideal and their activity is less than their concentration. The activity of the ions is given by the following equation:

$$a_i = \gamma_i \cdot c_i$$

where  $a_i$  is the activity of the ion,  $\gamma_i$  is the activity coefficient, and  $c_i$  is the concentration of the ion.

$$a_i = \gamma_i \cdot c_i$$



where,

$\Delta$  = standard deviation in energy loss (ergs)  
 $M$  = weight of particle (g.)  
 $t$  = thickness of stopping medium (g/cm<sup>2</sup>)

Substituting data for Ni foil of thickness 0.00006"

(equivalent to 1.13 mg/cm<sup>2</sup>) yields:

$$\begin{aligned}\Delta_{Ni}^2 &= 2.11 \times 10^{-16} \text{ ergs}^2 \\ &= 0.325 \times 10^{-4} \text{ Mev.}^2 \\ \Delta_{Ni} &= 0.0091 \text{ Mev.}\end{aligned}$$

For the gas from window to reaction volume the average distance is 1.82 cm. At atmospheric pressure one centimeter of the gas is equivalent to  $1.78 \times 10^{-5}$  g/cm<sup>2</sup>. For 1.82 cm. of gas at 75 mm. pressure we find the thickness to be:

$$1.82 \times 1.78 \times 10^{-5} \times \frac{75}{760} = 3.20 \times 10^{-4} \text{ g/cm}^2.$$

Substituting this into the formula we get for the gas:

$$\begin{aligned}\Delta_A^2 &= 0.143 \times 10^{-16} \text{ ergs}^2 \\ &= 0.0559 \times 10^{-4} \text{ Mev}^2 \\ \Delta_A &= 0.00236 \text{ Mev.}\end{aligned}$$

We may assume from the geometry of the reaction volume that more than 50% of the reaction takes place in a geometrical 50% zone straddling the mid-point of the target. Therefore, if the extreme energy spread in the target is 23 kev. (for initial beam energy of 1 Mev.) we

above.

A standard deviation in energy from 100 eV  
 is a standard deviation in energy from 100 eV  
 is a standard deviation in energy from 100 eV

Standard deviation in energy from 100 eV

Standard deviation in energy from 100 eV

$$\sigma_{\text{rel}} = \frac{\sigma}{\mu} = \frac{1.1 \times 10^{-16}}{1.1 \times 10^{-16}}$$

$$\sigma_{\text{rel}} = \frac{\sigma}{\mu} = \frac{1.1 \times 10^{-16}}{1.1 \times 10^{-16}}$$

$$\sigma_{\text{rel}} = \frac{\sigma}{\mu} = \frac{1.1 \times 10^{-16}}{1.1 \times 10^{-16}}$$

For the standard deviation in energy from 100 eV  
 is a standard deviation in energy from 100 eV  
 is a standard deviation in energy from 100 eV  
 is a standard deviation in energy from 100 eV  
 is a standard deviation in energy from 100 eV

$$1.1 \times 10^{-16} \pm \frac{1.1 \times 10^{-16}}{1.1 \times 10^{-16}} = 1.1 \times 10^{-16}$$

Standard deviation in energy from 100 eV

$$\sigma_{\text{rel}} = \frac{\sigma}{\mu} = \frac{1.1 \times 10^{-16}}{1.1 \times 10^{-16}}$$

$$\sigma_{\text{rel}} = \frac{\sigma}{\mu} = \frac{1.1 \times 10^{-16}}{1.1 \times 10^{-16}}$$

$$\sigma_{\text{rel}} = \frac{\sigma}{\mu} = \frac{1.1 \times 10^{-16}}{1.1 \times 10^{-16}}$$

Standard deviation in energy from 100 eV  
 is a standard deviation in energy from 100 eV  
 is a standard deviation in energy from 100 eV  
 is a standard deviation in energy from 100 eV  
 is a standard deviation in energy from 100 eV  
 is a standard deviation in energy from 100 eV  
 is a standard deviation in energy from 100 eV  
 is a standard deviation in energy from 100 eV

can assume that more than 50% of the elastically scattered protons will have an energy spread of less than 14 kev. If we consider this as a form of straggling we may combine this figure with the straggling due to the Ni window and that due to gas between window and target, and with the beam resolution of 5 kev. defined by the 1 mm. slit.

$$\Delta E = \left[ \Delta E_{\text{slit}}^2 + \Delta E_{\text{Ni}}^2 + \Delta E_A^2 + \Delta E_{\text{targ}}^2 \right]^{1/2}$$

$$= \left[ (25 + 82.5 + 5.6 + 196) \times 10^{-4} \right]^{1/2} \text{ Mev.}$$

$$= 0.0176 \text{ Mev.}$$

This is a conservative value for the most probable experimental resolution attained in the elastic scattering reaction. If the mean energy at the target is 0.806 Mev., the experimental resolution is therefore 2.2%.

Curve II of Figure 10 is the mean energy of the reaction vs. the beam energy.

Curve III of Figure 10 is the mean energy of elastically scattered protons reaching the sensitive volume of the counter. The sensitive volume relative to target is indicated on the range curve of Figure 9. This shows that an elastically scattered proton with an energy of 0.815 Mev. will just reach the sensitive volume at a pressure of 75 mm. Hg and that a scattered proton of 1.020 Mev. energy will reach the extreme limit of the sensitive volume. Since

There is a large number of people who are interested in the work of the Commission, and who are willing to help in any way they can. It is the duty of the Commission to make use of all the help that is offered, and to make the work as efficient as possible. The Commission is grateful to all those who have helped it in the past, and it trusts that it will be able to do so in the future.

$$\begin{aligned} \frac{1}{2} \left[ \begin{array}{c} 1 \\ 1 \\ 1 \\ 1 \end{array} \right] &= \frac{1}{2} \left[ \begin{array}{c} 1 \\ 1 \\ 1 \\ 1 \end{array} \right] \\ \frac{1}{2} \left[ \begin{array}{c} 1 \\ 1 \\ 1 \\ 1 \end{array} \right] &= \frac{1}{2} \left[ \begin{array}{c} 1 \\ 1 \\ 1 \\ 1 \end{array} \right] \end{aligned}$$

...the ... ..

have all of which is the main object of this

the Bragg ionization curve shows that the major portion of ionization of a charged particle travelling through a gas is near the end of its track, the particles with an initial reaction energy of 0.9 to 1.0 Mev. will be most efficiently counted at a pressure of 75 mm. Hg. This is the condition desired for investigating a resonance level near 0.900 Mev.

The first indication came about three weeks before  
the beginning of the summer vacation. I received a letter  
from the school, dated July 1st, 1900, in which it was  
stated that the school would be closed for the summer  
from July 1st to July 15th. I was very glad to hear  
of this, as I had been thinking of going home for  
the summer. I had been thinking of going home for  
the summer for some time, but had been unable to do so  
because of my work. I was very glad to hear of this,  
as I had been thinking of going home for the summer.

## V. EXPERIMENTAL RESULTS

Some of the experimental difficulties encountered were: (1) use of a nickel window required beam energies considerably in excess of energies desired in the reaction, (2) requirements of a moderate counting rate necessitated a small restricting aperture which cut down ion current approximately to 0.1 to 0.5 microcoulombs, (3) a 1 mm. slit for modest beam resolution combined with the restricting beam aperture required some finesse in aligning apparatus, and (4) gas pressure in the reaction and counting chambers had to be reduced to 50 mm. (Hg) pressure in order to raise the minimum energy of scattered protons reaching the sensitive volume. The extent of the sensitive volume at 50 mm. (Hg) has been added to the range-energy curve in Figure 9 in addition to the delineation of this region for 75 mm. (Hg) pressure. With this pressure the minimum energy scattered protons, which reach the sensitive volume, is 375 kev., and the energy of protons which just reach the far end of the sensitive volume is 780 kev. This means that protons which are scattered with an energy of greater than 780 kev. will produce slightly less ionization than those just below the 780 kev. level. This was found to be true in actual operation; and consequently, amplifier gain had to





be set up to about 14 in order that pulses would be large enough to insure counting all protons with a fixed bias voltage.

Two runs were made counting the scattered protons from argon gas at 50 mm. (Hg) pressure. Run #1 was made over the range of incident proton energies from 890 kev. to 1100 kev. inclusive. The data for this run are plotted in Figure 11. This curve shows a definite anomaly at 908 Kev. An arbitrary Coulomb scattering curve is superimposed showing a definite rising trend away from pure Coulomb scattering. This can be attributed largely to a nuclear scattering of the hard sphere type.

The Coulomb cross-section per unit solid angle is:

$$\sigma_c = \left[ \frac{2Ze^2}{4E} \right]^2 \cdot \frac{1}{\sin^4\left(\frac{\theta}{2}\right)}$$

$$\text{where } E = \frac{1}{2} \mu v^2 \quad (\text{ergs})$$

$$\begin{aligned} \mu &= \text{reduced mass of proton} \\ &= 1.63 \times 10^{-24} \text{ g.} \end{aligned}$$

The cross-section per unit solid angle due to a hard sphere type of scattering is:

$$\sigma_p = \frac{\lambda^2}{\pi} \sin^2\left(\frac{2\pi a}{\lambda}\right)$$

$$\text{where } \lambda = \frac{h}{\mu v}$$

$$\begin{aligned} a &= \text{interacting distances between nuclei} \\ &= 1.5 \text{ \AA}^{1/2} \times 10^{-13} \text{ cm.} \\ &= 5.12 \times 10^{-13} \text{ cm.} \end{aligned}$$

be not be so about it in order that we may be able to

[illegible]

$$\frac{1}{(1-\alpha)^2} \left[ \frac{1}{1-\alpha} \right]$$

(кратко)  $\frac{1}{2} \approx 0,5$

01 x 80.1 =

$$\left(\frac{\pi}{\lambda}\right)^2 \sin^2 \theta = \frac{\lambda}{\pi} = \frac{1}{\lambda}$$

*[Faint handwritten notes]*

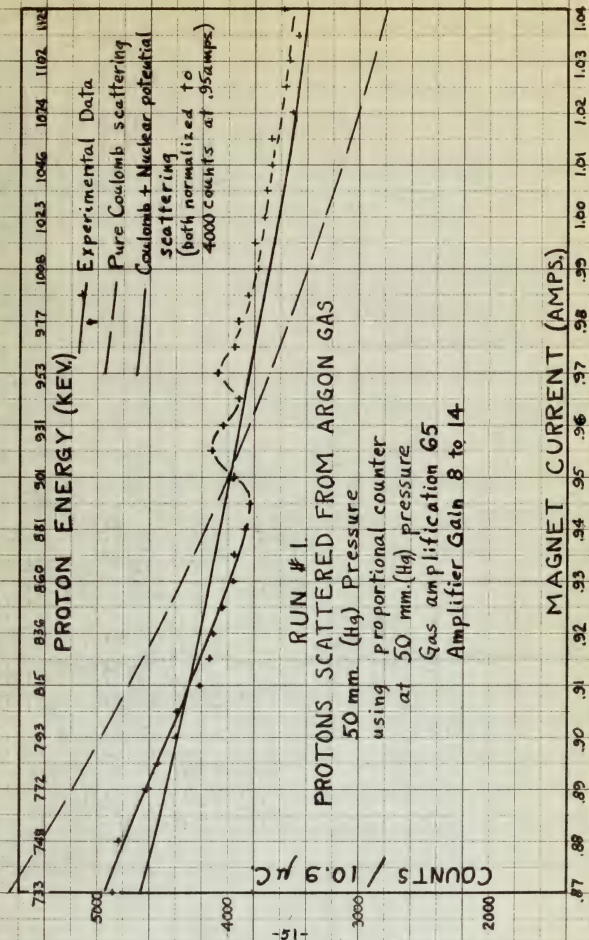


FIGURE 11.



If we neglect interference between Coulomb and nuclear potential scattering and attribute the total cross-section to a sum of the two effects,

$$\sigma = \sigma_c + \sigma_p$$

Now, the number of collected scattered particles counted in a solid angle of  $1/3144$  steradians is:

$$n(\theta) = n_0 N t \sigma / 3144$$

where  $n_0$  = number of incident particles

$N$  = number of atoms / cc.

$t$  = thickness of target (cm.)

$t$  is the only parameter not known with any degree of accuracy, but the shape of the scattering section of the gaseous target is that of a narrow cone intersecting a narrow cylinder at an angle of  $30^\circ$ . The extreme thickness of target section is 1.00 cm., but the effective thickness is somewhere between 0.25 and 0.50 cm. If we assume this effective thickness to be 0.366 cm. the number of collected scattered particles at an energy of 500 kev. is 4000 per 10.9 microcoulombs. These conditions then represent the existing conditions at the cross-over of the anomaly.

Using this value of  $t = 0.366$  cm. and other experimental conditions, the values of  $\sigma$  and  $n(\theta)$  were computed and tabulated in Table V. These assumptions are not considered to be out of line from most probable circumstances, and it will be noted that a plot of  $n(\theta)$  for various ener-

It is a very common mistake to suppose that the  
 only way of getting the best results is to  
 use the most expensive materials.

7 1 2 3 4

There are many other things which are  
 of great importance in the study of  
 the history of the world.

There are a number of things which are  
 of great importance in the study of  
 the history of the world.

There are a number of things which are  
 of great importance in the study of  
 the history of the world. There are a  
 number of things which are of great  
 importance in the study of the history  
 of the world. There are a number of  
 things which are of great importance  
 in the study of the history of the  
 world. There are a number of things  
 which are of great importance in the  
 study of the history of the world.

There are a number of things which are  
 of great importance in the study of  
 the history of the world. There are a  
 number of things which are of great  
 importance in the study of the history  
 of the world. There are a number of  
 things which are of great importance  
 in the study of the history of the  
 world. There are a number of things  
 which are of great importance in the  
 study of the history of the world.

gies falls very close to the experimental curve obtained except for the anomaly.

From a calibration run on a LiF target the proton energy at the cross-over of the anomaly is 908 kev. Experimental resolution of only about 20 kev. prevents an accurate location of the maximum and minimum points of the anomaly.

This result agrees well with the resonance level of 900 kev. found in argon by Broström, Hans, and Koch<sup>21</sup> in 1948. It demonstrates also that anomalies in elastic scattering of protons may be detected by this method of using a proportional counter even for atoms with Z-number up to 18.

A second run was made which verifies not only the existence of the anomaly at 908 kev. but a smaller anomaly reappears and is suggested as being superimposed on the principal one at an energy of about 945 kev. There was apparently a shift in magnet calibration between the first run and the second; but the energy spread in the anomaly and the energy difference between the two anomalies is the same. The first calibration on the LiF target is assumed correct. The second run is shown in Figure 12. A very slight variation in counting rate is noted but this may be due to inaccuracy in adjusting the gas pressure in the chamber.

When this test is made by the appropriate test machine, the results are usually.

From a comparison of the test results with the results of the test of the same test of the same test, it is found that the results of the test of the same test of the same test are in good agreement with the results of the test of the same test of the same test.

This result agrees well with the results of the test of the same test of the same test, and it is found that the results of the test of the same test of the same test are in good agreement with the results of the test of the same test of the same test.

A second run was made which verified not only the results of the first run but also the results of the second run. It is found that the results of the test of the same test of the same test are in good agreement with the results of the test of the same test of the same test.



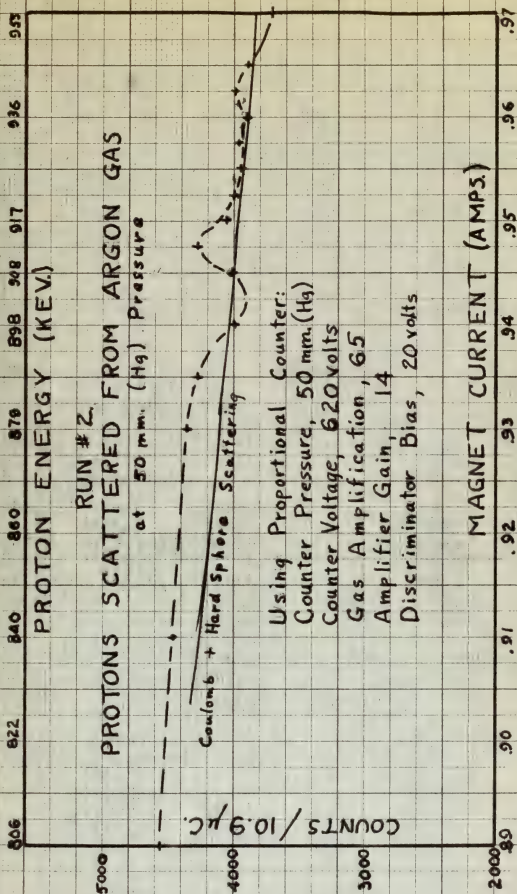
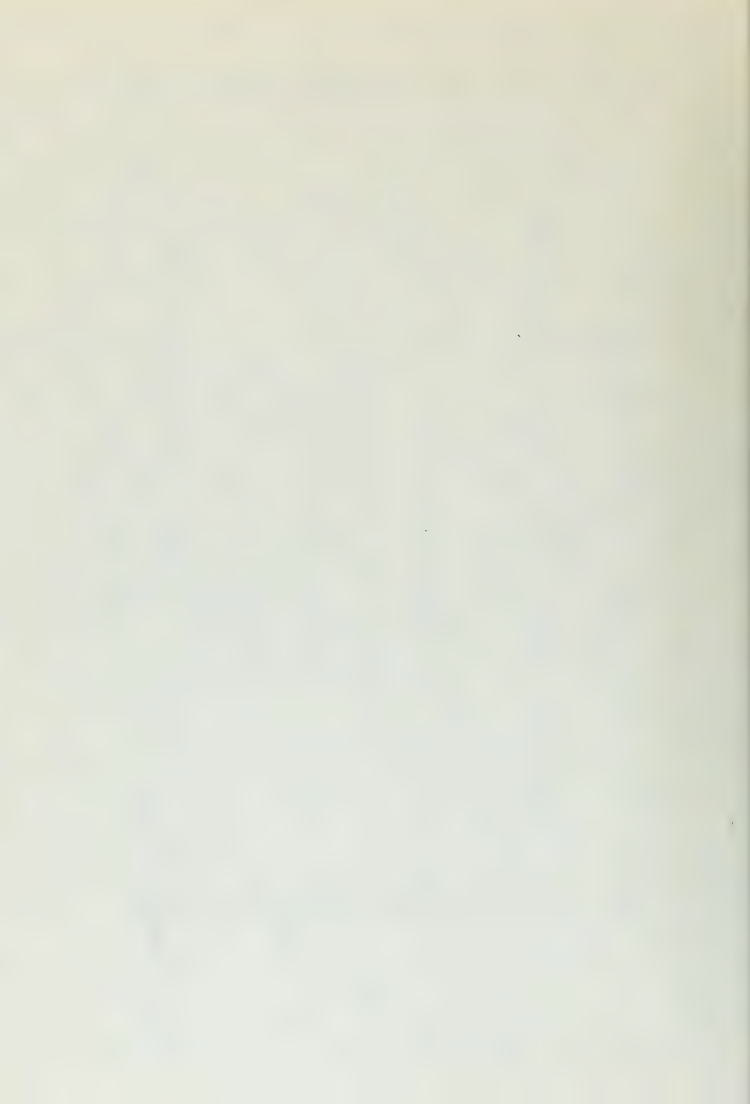


FIGURE 12.



The magnet calibration is indicated on Figures 11 and 12 with the anomaly located at 908 kev. in Figure 12.

A discriminator curve on scattered protons at energy of 890 kev. at the port of the proportional counter is shown in Figure 13.

### Conclusions.

(1) A resonance level in  $K^{41}$  has been located by means of proton bombardment of  $K^{40}$  and observation of an anomaly in the elastic scattering places this level at a proton energy of 908 kev. ( $\pm 10$  kev.)

(2) The feasibility of using a proportional counter to observe anomalies in the elastic scattering of a gas has been demonstrated.

(3) Elastic scattering in  $K^{40}$  at energies between 710 and 1133 kev. and at a laboratory scattering angle of  $180^\circ$  follows closely that predicted from a computation of the differential cross-sections due to superposition of Coulomb scattering and scattering from an impenetrable sphere.

The present situation is indicated in Figure 11. It is also the energy level of the ion in Figure 11. A comparison with the previous results is shown in Figure 12.

### Conclusions

(1) The present results in Figure 11 show that the energy level of the ion is  $10 \pm 1$  eV and the energy level of the electron is  $10 \pm 1$  eV.

(2) The energy level of the ion is  $10 \pm 1$  eV.

(3) The energy level of the electron is  $10 \pm 1$  eV.

(4) The energy level of the ion is  $10 \pm 1$  eV.

(5) The energy level of the electron is  $10 \pm 1$  eV.

(6) The energy level of the ion is  $10 \pm 1$  eV.

(7) The energy level of the electron is  $10 \pm 1$  eV.

(8) The energy level of the ion is  $10 \pm 1$  eV.

(9) The energy level of the electron is  $10 \pm 1$  eV.

(10) The energy level of the ion is  $10 \pm 1$  eV.

(11) The energy level of the electron is  $10 \pm 1$  eV.

(12) The energy level of the ion is  $10 \pm 1$  eV.

(13) The energy level of the electron is  $10 \pm 1$  eV.

(14) The energy level of the ion is  $10 \pm 1$  eV.

(15) The energy level of the electron is  $10 \pm 1$  eV.

(16) The energy level of the ion is  $10 \pm 1$  eV.

(17) The energy level of the electron is  $10 \pm 1$  eV.

(18) The energy level of the ion is  $10 \pm 1$  eV.

(19) The energy level of the electron is  $10 \pm 1$  eV.

(20) The energy level of the ion is  $10 \pm 1$  eV.

# PROTONS SCATTERED FROM ARGON GAS

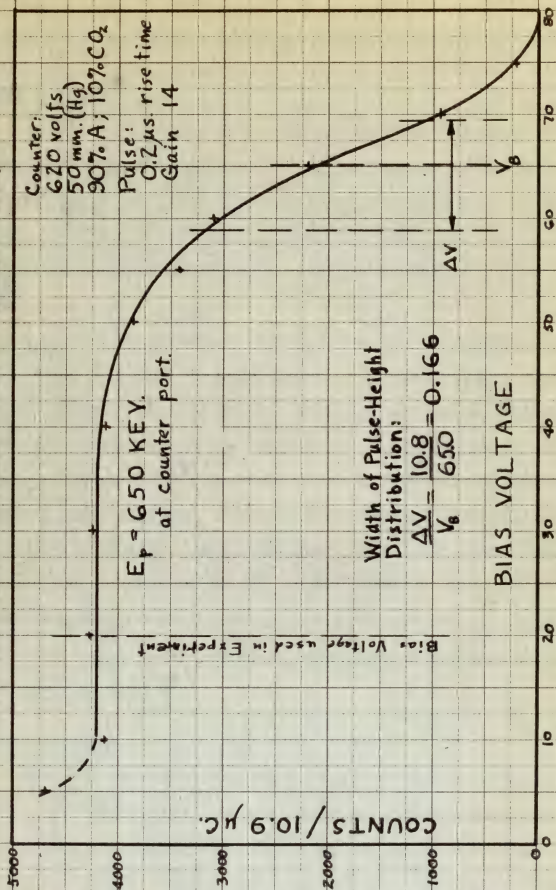


FIGURE 13.



## VI. SUGGESTIONS FOR FUTURE EXPERIMENTS

### Solid Targets.

As stated in Section I, one of the difficulties of using the present apparatus for solid targets is that visual observation of the beam is obstructed and alignment is extremely difficult especially since the very core of the proton beam must pass through a collimator of only 0.1" diameter.

A slight modification can be made by constructing a movable mounting for a solid target on a small shaft inserted through the wall of the reaction chamber or Faraday cage, pieces (2) and (3) of Figure 5. A vacuum seal gland would, of course, be necessary to avoid loss of pressure or vacuum in the chamber. With this modification, a solid target could be mounted, the apparatus closed and evacuated, and with the target swung out of the line of sight, the beam could be visually monitored and the apparatus aligned. Then, the target could be swung back into the proper position for bombardment.

### Gaseous Targets.

With the use of a thin mica window over the entry port of the counting chamber, it would be possible to have one gas mixture in the proportional counter and another in the reaction chamber. Naturally, separate gas filling connec-

THE UNIVERSITY OF CHICAGO

IN THE CITY OF CHICAGO, I, the undersigned, do hereby certify that

the following is a true and correct copy of the original as the same appears in the records of the University of Chicago, and that the same is a true and correct copy of the original as the same appears in the records of the University of Chicago, and that the same is a true and correct copy of the original as the same appears in the records of the University of Chicago.

I, the undersigned, do hereby certify that the following is a true and correct copy of the original as the same appears in the records of the University of Chicago, and that the same is a true and correct copy of the original as the same appears in the records of the University of Chicago, and that the same is a true and correct copy of the original as the same appears in the records of the University of Chicago.

THE UNIVERSITY OF CHICAGO

With the use of a fair and honest mind, the undersigned do hereby certify that the following is a true and correct copy of the original as the same appears in the records of the University of Chicago, and that the same is a true and correct copy of the original as the same appears in the records of the University of Chicago, and that the same is a true and correct copy of the original as the same appears in the records of the University of Chicago.



and a vacuum connection would have to be incorporated for the reaction chamber since it would be isolated from the counting chamber which now carries the gas filling connections and vacuum connection.

With this modification it would be possible to observe scattering and particle resonance reactions in different gases while still keeping the counting gas the same.

and a former member of the staff of the

for the purpose of being able to

and the matter of the matter of the

which is the matter of the matter of the

the matter of the matter of the matter of the

the matter of the matter of the matter of the

the matter of the matter of the matter of the

the matter of the matter of the matter of the

the matter of the matter of the matter of the

the matter of the matter of the matter of the

the matter of the matter of the matter of the

the matter of the matter of the matter of the

the matter of the matter of the matter of the

the matter of the matter of the matter of the

the matter of the matter of the matter of the

the matter of the matter of the matter of the

the matter of the matter of the matter of the

the matter of the matter of the matter of the

the matter of the matter of the matter of the

the matter of the matter of the matter of the

the matter of the matter of the matter of the

the matter of the matter of the matter of the

the matter of the matter of the matter of the

the matter of the matter of the matter of the

the matter of the matter of the matter of the

the matter of the matter of the matter of the

the matter of the matter of the matter of the

the matter of the matter of the matter of the

## VII. TABLES

TABLE I

Discriminator Curve on  $\text{Po}^{210}$  Internal Source.

Pressure 200 mm. Hg.  
Central Wire Voltage, +800 volts.  
Rise time, 0.2 microseconds.  
Using Model 205-B Preamplifier.  
Amplifier Gain, 2.

Discriminator	Alphas
Bias Voltage	Counts per minute
2	218
5	201
10	144
15	148
20	136
25	138
30	136
32	135
35	135
38	92
40	58
42	30
44	4
46	1
48	0

325. E.

1999, 2000, 2001, 2002, 2003, 2004, 2005, 2006, 2007, 2008, 2009, 2010, 2011, 2012, 2013, 2014, 2015, 2016, 2017, 2018, 2019, 2020, 2021, 2022, 2023, 2024, 2025, 2026, 2027, 2028, 2029, 2030, 2031, 2032, 2033, 2034, 2035, 2036, 2037, 2038, 2039, 2040, 2041, 2042, 2043, 2044, 2045, 2046, 2047, 2048, 2049, 2050, 2051, 2052, 2053, 2054, 2055, 2056, 2057, 2058, 2059, 2060, 2061, 2062, 2063, 2064, 2065, 2066, 2067, 2068, 2069, 2070, 2071, 2072, 2073, 2074, 2075, 2076, 2077, 2078, 2079, 2080, 2081, 2082, 2083, 2084, 2085, 2086, 2087, 2088, 2089, 2090, 2091, 2092, 2093, 2094, 2095, 2096, 2097, 2098, 2099, 2100, 2101, 2102, 2103, 2104, 2105, 2106, 2107, 2108, 2109, 2110, 2111, 2112, 2113, 2114, 2115, 2116, 2117, 2118, 2119, 2120, 2121, 2122, 2123, 2124, 2125, 2126, 2127, 2128, 2129, 2130, 2131, 2132, 2133, 2134, 2135, 2136, 2137, 2138, 2139, 2140, 2141, 2142, 2143, 2144, 2145, 2146, 2147, 2148, 2149, 2150, 2151, 2152, 2153, 2154, 2155, 2156, 2157, 2158, 2159, 2160, 2161, 2162, 2163, 2164, 2165, 2166, 2167, 2168, 2169, 2170, 2171, 2172, 2173, 2174, 2175, 2176, 2177, 2178, 2179, 2180, 2181, 2182, 2183, 2184, 2185, 2186, 2187, 2188, 2189, 2190, 2191, 2192, 2193, 2194, 2195, 2196, 2197, 2198, 2199, 2200, 2201, 2202, 2203, 2204, 2205, 2206, 2207, 2208, 2209, 2210, 2211, 2212, 2213, 2214, 2215, 2216, 2217, 2218, 2219, 2220, 2221, 2222, 2223, 2224, 2225, 2226, 2227, 2228, 2229, 2230, 2231, 2232, 2233, 2234, 2235, 2236, 2237, 2238, 2239, 2240, 2241, 2242, 2243, 2244, 2245, 2246, 2247, 2248, 2249, 2250, 2251, 2252, 2253, 2254, 2255, 2256, 2257, 2258, 2259, 2260, 2261, 2262, 2263, 2264, 2265, 2266, 2267, 2268, 2269, 2270, 2271, 2272, 2273, 2274, 2275, 2276, 2277, 2278, 2279, 2280, 2281, 2282, 2283, 2284, 2285, 2286, 2287, 2288, 2289, 2290, 2291, 2292, 2293, 2294, 2295, 2296, 2297, 2298, 2299, 2300, 2301, 2302, 2303, 2304, 2305, 2306, 2307, 2308, 2309, 2310, 2311, 2312, 2313, 2314, 2315, 2316, 2317, 2318, 2319, 2320, 2321, 2322, 2323, 2324, 2325, 2326, 2327, 2328, 2329, 2330, 2331, 2332, 2333, 2334, 2335, 2336, 2337, 2338, 2339, 2340, 2341, 2342, 2343, 2344, 2345, 2346, 2347, 2348, 2349, 2350, 2351, 2352, 2353, 2354, 2355, 2356, 2357, 2358, 2359, 2360, 2361, 2362, 2363, 2364, 2365, 2366, 2367, 2368, 2369, 2370, 2371, 2372, 2373, 2374, 2375, 2376, 2377, 2378, 2379, 2380, 2381, 2382, 2383, 2384, 2385, 2386, 2387, 2388, 2389, 2390, 2391, 2392, 2393, 2394, 2395, 2396, 2397, 2398, 2399, 2400, 2401, 2402, 2403, 2404, 2405, 2406, 2407, 2408, 2409, 2410, 2411, 2412, 2413, 2414, 2415, 2416, 2417, 2418, 2419, 2420, 2421, 2422, 2423, 2424, 2425, 2426, 2427, 2428, 2429, 2430, 2431, 2432, 2433, 2434, 2435, 2436, 2437, 2438, 2439, 2440, 2441, 2442, 2443, 2444, 2445, 2446, 2447, 2448, 2449, 2450, 2451, 2452, 2453, 2454, 2455, 2456, 2457, 2458, 2459, 2460, 2461, 2462, 2463, 2464, 2465, 2466, 2467, 2468, 2469, 2470, 2471, 2472, 2473, 2474, 2475, 2476, 2477, 2478, 2479, 2480, 2481, 2482, 2483, 2484, 2485, 2486, 2487, 2488, 2489, 2490, 2491, 2492, 2493, 2494, 2495, 2496, 2497, 2498, 2499, 2500, 2501, 2502, 2503, 2504, 2505, 2506, 2507, 2508, 2509, 2510, 2511, 2512, 2513, 2514, 2515, 2516, 2517, 2518, 2519, 2520, 2521, 2522, 2523, 2524, 2525, 2526, 2527, 2528, 2529, 2530, 2531, 2532, 2533, 2534, 2535, 2536, 2537, 2538, 2539, 2540, 2541, 2542, 2543, 2544, 2545, 2546, 2547, 2548, 2549, 2550, 2551, 2552, 2553, 2554, 2555, 2556, 2557, 2558, 2559, 2560, 2561, 2562, 2563, 2564, 2565, 2566, 2567, 2568, 2569, 2570, 2571, 2572, 2573, 2574, 2575, 2576, 2577, 2578, 2579, 2580, 2581, 2582, 2583, 2584, 2585, 2586, 2587, 2588, 2589, 2590, 2591, 2592, 2593, 2594, 2595, 2596, 2597, 2598, 2599, 2600, 2601, 2602, 2603, 2604, 2605, 2606, 2607, 2608, 2609, 2610, 2611, 2612, 2613, 2614, 2615, 2616, 2617, 2618, 2619, 2620, 2621, 2622, 2623, 2624, 2625, 2626, 2627, 2628, 2629, 2630, 2631, 2632, 2633, 2634, 2635, 2636, 2637, 2638, 2639, 2640, 2641, 2642, 2643, 2644, 2645, 2646, 2647, 2648, 2649, 2650, 2651, 2652, 2653, 2654, 2655, 2656, 2657, 2658, 2659, 2660, 2661, 2662, 2663, 2664, 2665, 2666, 2667, 2668, 2669, 2670, 2671, 2672, 2673, 2674, 2675, 2676, 2677, 2678, 2679, 2680, 26

TABLE II

EXPERIMENTAL MEASUREMENTS

Nickel Window to Reaction Volume:

Minimum	1.30 cm.
Maximum	2.33 cm.
Mean	1.82 cm.

Reaction Volume to Sensitive Volume of Proportional Counter:

Minimum	9.4 cm.
Maximum	10.4 cm.
Mean	9.9 cm.

Center of Target Volume to:

Near End of Sensitive Volume	9.9 cm.
Far End of Sensitive Volume	26.9 cm.

Length of Sensitive Volume: 17.0 cm.

Length of Reaction Collimator: 4.6 cm.

Diameter of Collimator Ports: 0.06" (0.162 cm.)

Thickness of Nickel Foil Window: 0.00005" (0.000127 cm.)

Laboratory Scattering Angle:  $150^{\circ} \pm 1.9^{\circ}$

Diameter of Beam Aperture: 0.1" (2.54 mm.)

Width of Beam Slit: 1 mm.

1946

TABLE III

Computation of Reaction Energy of Protons ( $E_m$ )

$E_{beam}$ (kev.)	900	1000	1100	1200
$E_{foil}$ (kev.)	745	855	965	1070
Range at foil (cm.)	1.65	2.03	2.42	2.86
$\Delta R_1$ (1.03 cm.)	.08	.08	.08	.08
$R_1$ (cm.)	1.57	1.95	2.35	2.78
$\Delta R_2$ (2.33 cm.)	.15	.15	.15	.15
$R_2$ (cm.)	1.80	1.98	2.28	2.71
$E_1$ (kev.)	718	830	940	1050
$E_2$ (kev.)	696	812	922	1033
$\Delta E$ (kev.)	22	18	18	17
$\Delta R_m$ (1.82 cm.)	.12	.12	.12	.12
$R_m$ (cm.)	1.53	1.81	2.31	2.74
$E_m$ (kev.)	706	820	931	1042

$\Delta R_{1,2}$  are minimum and maximum thickness of gas in chamber at 50 mm. (Hg) pressure reduced to equivalent range at 760 mm.

Values of  $E_{foil}$  are plotted as Curve I in Figure 10.

Values of  $E_m$  are plotted as Curve II in Figure 10.

# TABLE I

TABLE I. Summary of the experimental results for the reaction  $\pi^+ p \rightarrow \pi^+ \pi^+ p$  at 190 GeV/c.

Run	Beam	Target	Angle	Yield
1901	190	190	190	190
1902	190	190	190	190
1903	190	190	190	190
1904	190	190	190	190
1905	190	190	190	190
1906	190	190	190	190
1907	190	190	190	190
1908	190	190	190	190
1909	190	190	190	190
1910	190	190	190	190
1911	190	190	190	190
1912	190	190	190	190
1913	190	190	190	190
1914	190	190	190	190
1915	190	190	190	190
1916	190	190	190	190
1917	190	190	190	190
1918	190	190	190	190
1919	190	190	190	190
1920	190	190	190	190

TABLE I. Summary of the experimental results for the reaction  $\pi^+ p \rightarrow \pi^+ \pi^+ p$  at 190 GeV/c. The table shows the beam energy, target material, angle, and yield for each run. The beam energy is 190 GeV/c, the target material is 190, the angle is 190, and the yield is 190. The table is organized into four columns: Run, Beam, Target, Angle, and Yield. The runs are numbered from 1901 to 1920. The beam energy is 190 GeV/c, the target material is 190, the angle is 190, and the yield is 190. The table is organized into four columns: Run, Beam, Target, Angle, and Yield. The runs are numbered from 1901 to 1920. The beam energy is 190 GeV/c, the target material is 190, the angle is 190, and the yield is 190.



TABLE IV.

Energies of Elastically Scattered Protons at Entry Port  
of Counter ( $E_c$ )

$E_b$ (keV.)	900	1000	1100	1200
$E_m$ (Table III)	706	820	931	1042
$E_T$ ( $E_m \times 0.975$ )	689	800	909	1018
$R_T$ (cm.)	1.47	1.83	2.22	2.64
$\Delta R_1$ (9.4 cm.)	.62	.62	.62	.62
$R_1$ (cm.)	.85	1.21	1.60	2.02
$\Delta R_2$ (10.4 cm.)	.63	.68	.68	.68
$R_2$ (cm.)	.79	1.15	1.54	1.95
$E_1$ (keV.)	465	601	730	855
$E_2$ (keV.)	440	568	707	830
$\Delta E$ (keV.)	25	24	23	23
$\Delta R_3$ (9.9 cm.)	.65	.65	.65	.65
$R_3$ (cm.)	.82	1.10	1.57	1.99
$E_3$ (keV.)	452	593	720	842

$\Delta R_{1,2}$  are minimum and maximum distance from target to entry port of counter reduced to 760 mm (Hg) pressure as in Table III.

Values of  $E_3$  are plotted as Curve III in Figure 10.



TABLE V

Theoretical No. of Backscattered Protons into Solid Angle of  
1/3144 at an angle of 150°

E (Mev.)	0.700	0.800	0.900	1.000	1.100
E ( x 10 <sup>6</sup> ergs)	1.12	1.23	1.44	1.60	1.76
v ( x 10 <sup>-9</sup> cm/s)	1.17	1.25	1.33	1.40	1.47
$\lambda$ ( x 10 <sup>-12</sup> cm)	3.46	3.24	3.04	2.89	2.76
$\frac{2\pi A}{\lambda}$ (rad.)	.932	.994	1.060	1.114	1.167
$\frac{2\pi A}{\lambda}$ (degrees)	53.6°	56.95°	60.75°	63.8°	66.9°
$\sin^2(\frac{2\pi A}{\lambda})$	.644	.702	.761	.805	.846
$\frac{\lambda^2}{\pi}$ (barns)	3.92	3.35	2.95	2.66	2.43
$\sigma_p$ (barns)	2.46	2.34	2.26	2.14	2.05
$\sigma_e$ (barns)	.99	.75	.60	.48	.40
$\sigma$ (barns)	3.45	3.09	2.86	2.62	2.45
n (θ)	4820	4320	4000	3670	3430

$$\sigma_e = \frac{\lambda^2}{\pi} \sin^2 \left( \frac{2\pi A}{\lambda} \right)$$

$$\sigma_e = \left[ \frac{2\pi e^2}{h^2 v} \right]^2 \frac{1}{\sin^4 \left( \frac{\theta}{2} \right)}$$

$$\sigma = \sigma_p + \sigma_e$$

$$n(\theta) = n_0 N t \sigma / 3144$$

$$t = 0.366 \text{ cm.}$$

$$n_0 = 6.80 \times 10^{13} \text{ protons/10.9}$$

$$N = 1.77 \times 10^{17} \text{ atoms/cc.}$$



TABLE VI

Discriminator Data on Scattered Protons.

$E_0 = 650$  kev. at counter port. Counter pressure, 50 mm (Hg).

Counter voltage, +620 volts

Gas: 90% A; 10%  $\text{CO}_2$

Rise time, 0.2  $\mu\text{sec}$ .

Amplifier Gain, 14

<u>Bias Voltage</u>	<u>Counts/ 10.9 nC.</u>
5	4697
10	4132
20	4271
30	4240
40	4122
50	3851
55	3402
60	3100
65	2199
70	938
75	247
80	8

• 2005 12, 6. 2005 12, 6. 2005 12, 6.

# REFERENCES

1. Born. Z. Physik 38, 803 (1926). Also Landé.  
Quantum Mechanics, p.94, Pitman Pub. Corp. (1961).
2. Biecke and Marshal. Phys. Rev. 63, 86 (1948).
3. Wilkins. Phys. Rev. 60, 365 (1941).
4. Davis and Hafner. Phys. Rev. 73, 1848 (1949).
5. Powell, May, Chadwick, and Piekavance. Nature 145,  
393 (1940).
6. Fulbright and Bush. Phys. Rev. 74, 1823 (1949).
7. Rhoderick. Proc. Roy. Soc. London A, 201, 343 (1950).
8. Rutherford, Chadwick, and Ellis. Radiations from Radio-  
active Substances. (1930). Also Bessel. Atomic Physics  
Rinehart (1946).
9. Crookford and Walton. Nature 129, 649 (1932).
10. Gliphant, Kempton, and Rutherford. Proc. Roy. Soc. 149,  
406 (1938).
11. Neuert. Phys. Zeit. 36, 629 (1935).
12. Kirchner and Neuert. Phys. Zeit. 36, 84 (1935).
13. Gliphant, Kempton, and Rutherford. Proc. Roy. Soc. 150,  
241 (1935).
14. Dea and Gilbert. Proc. Roy. Soc. 154, 279 (1936).
15. Henderson, Livingston, and Lawrence. Phys. Rev. 46, 38  
(1934).
16. Halliday. Introductory Nuclear Physics. Wiley (1950).
17. Hornyak, Lauritsen, Morrison, and Fowler. Rev. Mod.  
Phys. 22, 291, (1950).

CONTENTS

1. <u>General Introduction</u> .....	1
2. <u>The History of the Church in the Middle Ages</u> .....	15
3. <u>The History of the Church in the Modern Period</u> .....	35
4. <u>The History of the Church in the Future</u> .....	55
5. <u>The History of the Church in the Present</u> .....	75
6. <u>The History of the Church in the Past</u> .....	95
7. <u>The History of the Church in the World</u> .....	115
8. <u>The History of the Church in the Nation</u> .....	135
9. <u>The History of the Church in the Community</u> .....	155
10. <u>The History of the Church in the Family</u> .....	175
11. <u>The History of the Church in the Individual</u> .....	195
12. <u>The History of the Church in the Church</u> .....	215
13. <u>The History of the Church in the Church</u> .....	235
14. <u>The History of the Church in the Church</u> .....	255
15. <u>The History of the Church in the Church</u> .....	275
16. <u>The History of the Church in the Church</u> .....	295
17. <u>The History of the Church in the Church</u> .....	315
18. <u>The History of the Church in the Church</u> .....	335
19. <u>The History of the Church in the Church</u> .....	355
20. <u>The History of the Church in the Church</u> .....	375



18. Allburger, and Hafner. The Properties of Atomic Nuclei. Brookhaven National Laboratory Pamphlet BNL-7-9 (1949).
19. Devons. Excited States of Nuclei. Cambridge Press. (1949).
20. Freeman and Baxter. Nature 162, 596 (1948).
21. Broström, Hans, and Kosh. Nature 162, 595 (1948).
22. Landé. Quantum Mechanics. Pitman (1951).
23. Wentzel. J. Physik 40, 590 (1936).
24. Gini. Isotopic Tracers and Nuclear Radiations. McGraw-Hill (1940).
25. Feshbach, Peaslee, and Weisskopf. Phys. Rev. 71, 145 (1947).
26. Brerar, Rosenfeld, Schluter. Nuclear Physics. Notes on a course given by Enrico Fermi. (1950).
27. Bethe. Rev. Mod. Phys. 9, 69 (1937).
28. Rose. Phys. Rev. 87, 968 (1940).
29. Bender, Shoemaker, Kaufmann, and Bourisane. Phys. Rev. 70, 273 (1949).
30. Mooring, Koester, Goldberg, Sakon, and Kaufmann. Phys. Rev. 94, 703 (Nov. 15, 1951).
31. Leubenstein and Leubenstein. Phys. Rev. 94, 18 (1951).
32. Koester. Phys. Rev. 95, 643 (Feb. 15, 1952).
33. A. B. Chilton. Master's Thesis. The Design and Construction of an Apparatus for Detection of Proton-Alpha Nuclear Reactions. Ohio State University. (1951)

174. Albuquerque, New Mexico: The University of New Mexico  
Library, Department of Anthropology  
1962-1963 (1963).
175. Various United States of America, Collection  
1962-1963.
176. Various of Mexico, Mexico City, 1962-1963.
177. Various, Mexico, 1962-1963, 1964-1965.
178. Various, Mexico, 1962-1963, 1964-1965.
179. Various, Mexico, 1962-1963, 1964-1965.
180. Various, Mexico, 1962-1963, 1964-1965.
181. Various, Mexico, 1962-1963, 1964-1965.
182. Various, Mexico, 1962-1963, 1964-1965.
183. Various, Mexico, 1962-1963, 1964-1965.
184. Various, Mexico, 1962-1963, 1964-1965.
185. Various, Mexico, 1962-1963, 1964-1965.
186. Various, Mexico, 1962-1963, 1964-1965.
187. Various, Mexico, 1962-1963, 1964-1965.
188. Various, Mexico, 1962-1963, 1964-1965.
189. Various, Mexico, 1962-1963, 1964-1965.
190. Various, Mexico, 1962-1963, 1964-1965.
191. Various, Mexico, 1962-1963, 1964-1965.
192. Various, Mexico, 1962-1963, 1964-1965.
193. Various, Mexico, 1962-1963, 1964-1965.
194. Various, Mexico, 1962-1963, 1964-1965.
195. Various, Mexico, 1962-1963, 1964-1965.
196. Various, Mexico, 1962-1963, 1964-1965.
197. Various, Mexico, 1962-1963, 1964-1965.
198. Various, Mexico, 1962-1963, 1964-1965.
199. Various, Mexico, 1962-1963, 1964-1965.
200. Various, Mexico, 1962-1963, 1964-1965.

- 34. W. E. L. Boyce. Master's Thesis. A Current Integrator.  
Ohio State University. (1952).
- 35. Hirschfelder and Magee. Phys. Rev. 73, 207 (1948).
- 36. Madsen and Venkateswarlu. Phys. Rev. 74, 1782 (1948).

34. W. E. L. Boyce. Master's Thesis. A Critical Investigation.  
Ohio State University. (1932).
35. Kirschleider and Magee. Phys. Rev. 55, 207 (1943).
36. Maden and Venkateswari. Phys. Rev. 54, 1928 (1943).
37. ...
38. ...
39. ...
40. ...
41. ...
42. ...
43. ...
44. ...
45. ...
46. ...
47. ...
48. ...
49. ...
50. ...
51. ...
52. ...
53. ...
54. ...
55. ...
56. ...
57. ...
58. ...
59. ...
60. ...
61. ...
62. ...
63. ...
64. ...
65. ...
66. ...
67. ...
68. ...
69. ...
70. ...
71. ...
72. ...
73. ...
74. ...
75. ...
76. ...
77. ...
78. ...
79. ...
80. ...
81. ...
82. ...
83. ...
84. ...
85. ...
86. ...
87. ...
88. ...
89. ...
90. ...
91. ...
92. ...
93. ...
94. ...
95. ...
96. ...
97. ...
98. ...
99. ...
100. ...

MAY 20  
JUN 3  
JUN 9  
MY 157

871  
871  
876  
4638

17236

Thesis  
D66

Dorsett

Investigation of  
proton induced reactions  
in light nuclei using  
proportional counter.

Thesis  
D66

Dorsett

17236

Investigation of proton induced re-  
actions in light nuclei using propor-  
tional counter.



thesD66missing  
Investigation of proton induced reaction



3 2768 002 00611 6

DUDLEY KNOX LIBRARY